ESAIM: M2AN 59 (2025) 3227–3247
https://doi.org/10.1051/m2an/2025088

ESAIM: Mathematical Modelling and Numerical Analysis
www.esaim-m2an.org

NUMERICAL ANALYSIS OF THE A-FORMULATION OF MAXWELL VARIATIONAL INEQUALITY

Feifei Jing[1,2], Xiaodi Zhang[3,*] and Weiying Zheng[4]

Abstract. In this work, we explore a Maxwell variational inequality arising from Bean's critical-state model in type-II superconductivity. Instead of the coupled electric and magnetic fields, we study an equivalent model based on the magnetic vector potential. The well-posedness of this transformed Maxwell variational inequality comes naturally from the hyperbolic Maxwell (quasi-)variational inequality arguments. We establish error estimates for both the spatially semi-discrete scheme and the fully discrete scheme. We propose two kinds of methods, the projection method and the regularization method, to solve the variational inequality problem. Two numerical experiments are reported to verify the theories and to investigate the physics of type-II superconductivity.

Mathematics Subject Classification. 35D30, 35M87, 49J40, 65M60.

Received July 25, 2024. Accepted October 11, 2025.

1. Introduction

Since the pioneering works of Bean [7, 8] and Kim [26], great progress have been made on the modeling, theoretical analysis, and numerical solutions of hyperbolic variational inequalities of electromagnetic problems. Duvaut and Lions went ahead the first study on hyperbolic variational inequalities in electromagnetism, and proved the existence and uniqueness of the strong solution to a hyperbolic Maxwell variational inequality of the first kind [11]. Milani extended their results to a time-dependent obstacle set [32, 33]. Prigozhin [38–40], Barrett and Prigozhin [2–6] studied the Bean critical state model governed by eddy current equations. In [34–36], the authors considered parabolic and elliptic variational inequalities of a p-curl type arising from the power law for eddy current equations. The corresponding model governed by full Maxwell's equations was studied in [22, 23]. Recently, Yousept revealed that the Bean critical-state model for high-temperature superconductors leads to a hyperbolic Maxwell variational inequality of the second kind [45]. A series of works are, respectively, focused

Keywords and phrases. Maxwell variational inequality, finite element method, error estimates, projection method, regularization method.

[1] School of Mathematics and Statistics and Xi'an Key Laboratory of Scientific Computation and Applied Statistics, Northwestern Polytechnical University, Xi'an 710129, Shaanxi, P.R. China.

[2] MOE Key Laboratory for Complexity Science in Aerospace, Northwestern Polytechnical University, Xi'an 710129, Shaanxi, P.R. China.

[3] School of Mathematics and Statistics, Zhengzhou University, Zhengzhou 450001, P.R. China.

[4] LSEC, NCMIS, Institute of Computational Mathematics and Scientific/Engineering Computing, Academy of Mathematics and Systems Science, Chinese Academy of Sciences, School of Mathematical Science, University of Chinese Academy of Sciences, Beijing 100190, P.R. China.

[*]Corresponding author: zhangxiaodi@lsec.cc.ac.cn

on shape optimization [28], optimal control problem [9,28,44,46], fully discrete schemes [41], Maxwell quasi-variational inequalities [17,49], the well-posedness and numerical analysis of electromagnetic obstacle problems [16,48], and adaptive edge element methods [43]. We also refer to the recent work [15] for numerical solutions of $\boldsymbol{H}(\mathbf{curl})$-elliptic hemivariational inequalities.

Let $T > 0$ be the final instant of time evolution, let $\Omega \subset \mathbb{R}^3$ be a bounded and simply connected domain with a connected boundary $\partial\Omega$, and it is filled with an open set $\overline{\Omega}_{\mathrm{sc}} \subset \Omega$, where Ω_{sc} represents a type-II high-temperature superconductor. Maxwell's equations with the Bean constitutive law for the electric field and the current density are given as follows

$$\begin{cases} \epsilon\, \partial_t \boldsymbol{E} - \mathbf{curl}\,(\mu^{-1}\boldsymbol{B}) + \boldsymbol{J} = \tilde{\boldsymbol{\ell}} & \text{in } \Omega \times (0,T), \\ \partial_t \boldsymbol{B} + \mathbf{curl}\,\boldsymbol{E} = 0 & \text{in } \Omega \times (0,T), \\ \boldsymbol{E} \times \boldsymbol{n} = 0 & \text{on } \partial\Omega \times (0,T), \\ \boldsymbol{E}(\cdot,0) = \boldsymbol{E}_0, \quad \boldsymbol{B}(\cdot,0) = \boldsymbol{B}_0 & \text{in } \Omega, \\ |\boldsymbol{J}(\boldsymbol{x},t)| \le j_c(\boldsymbol{x},t) & \text{for } a.e.\ (\boldsymbol{x},t) \in \Omega \times (0,T), \\ \boldsymbol{J}(\boldsymbol{x},t)\cdot \boldsymbol{E}(\boldsymbol{x},t) = j_c(\boldsymbol{x},t)|\boldsymbol{E}(\boldsymbol{x},t)| & \text{for } a.e.\ (\boldsymbol{x},t) \in \Omega \times (0,T). \end{cases} \tag{1}$$

Here $\boldsymbol{E} : \Omega \times (0,T) \to \mathbb{R}^3$ denotes the electric field, $\boldsymbol{B} : \Omega \times (0,T) \to \mathbb{R}^3$ the magnetic induction, $\boldsymbol{J} : \Omega \times (0,T) \to \mathbb{R}^3$ the current density, $\tilde{\boldsymbol{\ell}} : \Omega \times (0,T) \to \mathbb{R}^3$ the applied current source, and $j_c(\boldsymbol{x},t)$ the critical current. For a function $f(\boldsymbol{x},t)$, both $\dot{f}$ and $\partial_t f$ represent the first-order partial derivative of f with respect to t, furthermore, the time-variable t in the familiar $\boldsymbol{E}, \boldsymbol{B}, \boldsymbol{A}$ is left out most of time for simplicity.

The variational inequality of the second kind can be easily derived from (1) (cf. [14,32,45]):

$$\begin{aligned} \int_\Omega \Big[\epsilon\, \partial_t \boldsymbol{E}(t)\cdot(\boldsymbol{v} - \boldsymbol{E}(t)) + \mu^{-1}\partial_t \boldsymbol{B}(t)\cdot(\boldsymbol{w} - \boldsymbol{B}(t)) + \mu^{-1}\mathbf{curl}\,\boldsymbol{E}(t)\cdot\boldsymbol{w} - \mu^{-1}\boldsymbol{B}(t)\cdot\mathbf{curl}\,\boldsymbol{v}\Big]\,\mathrm{d}\boldsymbol{x} \\ + \int_\Omega \big(|\boldsymbol{v}| - |\boldsymbol{E}(t)|\big) j_c(\boldsymbol{x},t)\,\mathrm{d}\boldsymbol{x} \ge \int_\Omega \tilde{\boldsymbol{\ell}}(t)\cdot(\boldsymbol{v} - \boldsymbol{E}(t))\,\mathrm{d}\boldsymbol{x} \\ \text{for a.e. } t \in (0,T), \forall (\boldsymbol{v},\boldsymbol{w}) \in \boldsymbol{H}_0(\mathbf{curl}\,,\Omega) \times \boldsymbol{L}^2(\Omega). \end{aligned} \tag{2}$$

Here the critical value j_c is independent of $\boldsymbol{B}(t)$. If j_c depends on the magnetic induction, the mathematical model corresponds to a parabolic quasi-variational inequality (cf. [3,17,26,49]). We refer to [6] nonconforming finite element methods for such problem. The hyperbolic Maxwell variational inequality has been studied extensively in a series of works (cf. [28,41,45–48]). In [41], Winckler and Yousept proposed a fully discrete scheme for the Maxwell variational inequality with temperature effects. Usually, the electric field $\boldsymbol{E}$ and magnetic induction $\boldsymbol{B}$ are regarded as unknown variables of the problem.

The Gauss's law $\nabla\cdot\boldsymbol{B} = 0$ implies that there is no monopole of magnet. It is interesting to develop numerical schemes that can preserve this divergence-free condition on the discrete level [20,21]. The constraint $\nabla\cdot\boldsymbol{B} = 0$ implies the existence of a vector potential $\boldsymbol{A}$ which satisfies, upon using the second equation of (1) and the temporal gauge,

$$\boldsymbol{E} = -\partial_t \boldsymbol{A} \quad \text{and} \quad \boldsymbol{B} = \mathbf{curl}\,\boldsymbol{A} \quad \text{in } \Omega. \tag{3}$$

Then substituting (3) into the first equation of (1) leads to

$$\epsilon\, \partial_{tt}\boldsymbol{A} + \mathbf{curl}\,\left(\mu^{-1}\mathbf{curl}\,\boldsymbol{A}\right) - \boldsymbol{J} = \boldsymbol{\ell} := -\tilde{\boldsymbol{\ell}}.$$

In this work, we shall treat $\boldsymbol{A}$ as the main unknown variable and discretize it with the first-order edge element method. The discrete magnetic induction is defined by $\mathbf{curl}\,\boldsymbol{A}^h$ where $\boldsymbol{A}^h$ is the discrete solution. Naturally we obtain the conservation of magnetic induction, that is, $\operatorname{div}\boldsymbol{B}^h = 0$.

To set the initial value of $\boldsymbol{A}$, we utilize (3) and the third equation of (1). The initial condition $\boldsymbol{A}_0$ for $\boldsymbol{A}$ can be proposed by solving the following static problem

$$\begin{cases} \mathbf{curl}\,\boldsymbol{A}_0 = \boldsymbol{B}_0, \quad \operatorname{div}\boldsymbol{A}_0 = 0 & \text{in } \Omega, \\ \qquad\qquad\qquad \boldsymbol{A}_0 \times \boldsymbol{n} = 0 & \text{on } \partial\Omega. \end{cases} \tag{4}$$

From the vector potential theorem in Theorem 3.6 of [13], there exists a unique solution $\boldsymbol{A}_0$ to (4). The boundary condition for $\boldsymbol{A}$ can also be obtained as follows

$$\boldsymbol{A} \times \boldsymbol{n} = \boldsymbol{A}_0 \times \boldsymbol{n} - \int_0^t \boldsymbol{E} \times \boldsymbol{n}\,\mathrm{d}s = 0 \quad \text{on } \partial\Omega. \tag{5}$$

Conversely, the identity $\boldsymbol{E} = -\partial_t \boldsymbol{A}$ and the boundary condition $\boldsymbol{A} \times \boldsymbol{n} = 0$ for all $t \geq 0$ also imply $\boldsymbol{E} \times \boldsymbol{n} = 0$ on $\partial\Omega$ for all $t > 0$. The Maxwell system can be cast into a compact form

$$\begin{cases} \epsilon\,\partial_{tt}\boldsymbol{A} + \mathbf{curl}\,(\mu^{-1}\mathbf{curl}\,\boldsymbol{A}) - \boldsymbol{J} = \boldsymbol{\ell} & \text{in } \Omega \times (0,T), \\ \boldsymbol{A} \times \boldsymbol{n} = 0 & \text{on } \partial\Omega \times (0,T), \\ \partial_t \boldsymbol{A}(\cdot,0) = -\boldsymbol{E}_0, \quad \boldsymbol{A}(\cdot,0) = \boldsymbol{A}_0 & \text{in } \Omega, \\ |\boldsymbol{J}(\boldsymbol{x},t)| \leq j_c(\boldsymbol{x},t) & \text{for a.e. } (\boldsymbol{x},t) \in \Omega \times (0,T), \\ \boldsymbol{J}(\boldsymbol{x},t) \cdot \partial_t \boldsymbol{A}(\boldsymbol{x},t) + j_c(\boldsymbol{x},t)|\partial_t \boldsymbol{A}(\boldsymbol{x},t)| = 0 & \text{for a.e. } (\boldsymbol{x},t) \in \Omega \times (0,T). \end{cases} \tag{6}$$

Our research is focused on numerical analysis of the hyperbolic variational inequality of (6). This work makes a twofold contribution. We first investigate the well-posedness of the proposed Maxwell variational inequality, and explore error estimates for both a spatially semi-discrete scheme and a fully discrete scheme. To solve the discrete inequality problem, we propose a projection method and a regularization method. The numerical analysis for Maxwell variational inequality problems can be generalized to hemivariational inequality problems. We will address the issues in future works.

The rest of this paper is organized as follows. In Section 2, we introduce the Maxwell variational inequality based on (6) and establish its well-posedness. In Section 3, we propose a semi-discrete scheme based on finite element method for the variational inequality problem. Error estimate is obtained. In Section 4, we propose a fully discrete scheme for the problem and establish its stability and the first-order convergence rates both in time and space. In Section 5, we present two numerical algorithms for solving the variational inequality and report some numerical experiments. Throughout this paper, $C > 0$ denotes a generic constant independent of sensitive parameters, such as the time-step size τ and the mesh size h, and "$a \lesssim b$" stands for "$a \leq Cb$".

2. Variational form of the Maxwell inequality problem

The purpose of this section is to propose a variational formulation for the inequality problem. The well-posedness of the variational inequality problem will follow [17,45,49].

2.1. Function spaces

First we introduce some function spaces used in this paper. For a normed space X, $\|\cdot\|_X$ denotes its norm, X^* its topologically dual space, and $(\cdot,\cdot)_{X\times X^*}$ the duality paring between X^* and X. For a given integer m, $H^m(\Omega) := \{v \in L^2(\Omega) : \partial^{\boldsymbol{k}} v \in L^2(\Omega),\ \forall \boldsymbol{k} : k_1 + k_2 + k_3 \leq m\}$ denotes the standard Sobolev spaces, where $\boldsymbol{k} = (k_1, k_2, k_3)$ denotes the triple index and k_1, k_2, k_3 are nonnegative integers. The norm and semi-norm on $H^m(\Omega)$ are denoted by $\|v\|_{m,\Omega}$ and $|v|_{m,\Omega}$, respectively. For a nonnegative function $\alpha \in L^\infty(\Omega)$, $L^2_\alpha(\Omega)$ denotes the weighted L^2-space with the weighted scalar product $(\alpha\cdot,\cdot)_\Omega$ and norm $\|\cdot\|_{0,\Omega,\alpha}$. For simplicity, we drop the subscript Ω in the rest of this paper.

We shall also use the following spaces of vector-valued functions

$$
\begin{aligned}
\boldsymbol{H}(\mathbf{curl}\,,\Omega) &:= \left\{\boldsymbol{v} \in \boldsymbol{L}^2(\Omega) : \mathbf{curl}\,\boldsymbol{v} \in \boldsymbol{L}^2(\Omega)\right\},\\
\boldsymbol{H}_0(\mathbf{curl}\,,\Omega) &:= \{\boldsymbol{v} \in \boldsymbol{H}(\mathbf{curl}\,,\Omega) : \boldsymbol{v} \times \boldsymbol{n} = \mathbf{0} \text{ on } \partial\Omega\},\\
\boldsymbol{H}(\mathrm{div},\Omega) &:= \left\{\boldsymbol{v} \in \boldsymbol{L}^2(\Omega) : \mathrm{div}\,\boldsymbol{v} \in L^2(\Omega)\right\},\\
\boldsymbol{H}(\mathrm{div}\,0,\Omega) &:= \{\boldsymbol{v} \in \boldsymbol{H}(\mathrm{div},\Omega) : \mathrm{div}\,\boldsymbol{v} = 0\},\\
\boldsymbol{X}(\mathrm{div}\,0,\Omega) &:= \boldsymbol{H}_0\left(\mathbf{curl}\,,\Omega\right) \cap \boldsymbol{H}\left(\mathrm{div}\,0,\Omega\right),
\end{aligned}
$$

with the respective norms on $\boldsymbol{H}(\mathbf{curl}\,,\Omega)$,

$$
\|\boldsymbol{v}\|_{\mathbf{curl}} = \left(\|\boldsymbol{v}\|_0^2 + \|\mathbf{curl}\,\boldsymbol{v}\|_0^2\right)^{1/2}.
$$

Moreover, we shall also use the regular curl space

$$
\boldsymbol{H}^1(\mathbf{curl}\,,\Omega) = \left\{\boldsymbol{v} \in \boldsymbol{H}^1(\Omega) : \mathbf{curl}\,\boldsymbol{v} \in \boldsymbol{H}^1(\Omega)\right\}, \quad \|\boldsymbol{v}\|_{\boldsymbol{H}^1(\mathbf{curl}\,,\Omega)} = \left(\|\boldsymbol{v}\|^2_{\boldsymbol{H}^1(\Omega)} + \|\mathbf{curl}\,\boldsymbol{v}\|^2_{\boldsymbol{H}^1(\Omega)}\right)^{1/2}.
$$

2.2. Variational formulation

Define the bilinear form $a(\cdot,\cdot) : \boldsymbol{H}_0(\mathbf{curl}\,,\Omega) \times \boldsymbol{H}_0(\mathbf{curl}\,,\Omega) \to \mathbb{R}$ by

$$
a(\boldsymbol{u},\boldsymbol{v}) = \left(\mu^{-1}\mathbf{curl}\,\boldsymbol{u}, \mathbf{curl}\,\boldsymbol{v}\right).
$$

From [13, 18, 37], there exists a constant $\tilde{\alpha} > 0$ such that

$$
\|\mathbf{curl}\,\boldsymbol{v}\|_0 \geq \tilde{\alpha}\|\boldsymbol{v}\|_0 \quad \forall\,\boldsymbol{v} \in \boldsymbol{X}(\mathrm{div}\,0,\Omega). \tag{7}
$$

The semi-norm $\|\mathbf{curl}\,\cdot\|_0$ is equivalent to $\|\cdot\|_{\mathbf{curl}}$. An immediate consequence of (7) is

$$
\exists\,\kappa \in \mathbb{R}^+, \quad a(\boldsymbol{v},\boldsymbol{v}) \geq \kappa\|\boldsymbol{v}\|^2_{\mathbf{curl}} \quad \forall\,\boldsymbol{v} \in \boldsymbol{X}(\mathrm{div}\,0,\Omega). \tag{8}
$$

Now we derive the variational form of the transformed Maxwell model (6). For any $\boldsymbol{v} \in \boldsymbol{H}_0(\mathbf{curl}\,,\Omega)$, multiplying the first equation in (6) by $\boldsymbol{v} - \partial_t\boldsymbol{A} \in \boldsymbol{H}_0(\mathbf{curl}\,,\Omega)$ and using integration by parts, we obtain

$$
(\epsilon\,\partial_{tt}\boldsymbol{A}, \boldsymbol{v} - \partial_t\boldsymbol{A}) + \left(\mu^{-1}\mathbf{curl}\,\boldsymbol{A}, \mathbf{curl}\,(\boldsymbol{v} - \partial_t\boldsymbol{A})\right) + (-\boldsymbol{J}, \boldsymbol{v} - \partial_t\boldsymbol{A}) = (\boldsymbol{\ell}(t), \boldsymbol{v} - \partial_t\boldsymbol{A}).
$$

From the fourth and fifth constraint conditions in (6), we see that

$$
(-\boldsymbol{J}, \boldsymbol{v} - \partial_t\boldsymbol{A}) = (-\boldsymbol{J}, \boldsymbol{v}) + (\boldsymbol{J}, \partial_t\boldsymbol{A}) \leq \int_\Omega j_c(\boldsymbol{x},t)\cdot|\boldsymbol{v}|\,\mathrm{d}\boldsymbol{x} - \int_\Omega j_c(\boldsymbol{x},t)\cdot|\partial_t\boldsymbol{A}|\,\mathrm{d}\boldsymbol{x}.
$$

Define a functional $\varphi : [0,T] \times \boldsymbol{L}^1(\Omega) \to \mathbb{R}$ by $\varphi(t,\boldsymbol{v}) = \int_\Omega j_c(\boldsymbol{x},t)\cdot|\boldsymbol{v}|\,\mathrm{d}\boldsymbol{x}$. We are now led to the following Maxwell variational inequality of the second kind.

Problem 2.1. Find $\boldsymbol{A} \in W^{2,\infty}(0,T;\boldsymbol{L}^2(\Omega)) \cap W^{1,\infty}(0,T;\boldsymbol{H}_0(\mathbf{curl}\,,\Omega))$ such that

$$
\begin{aligned}
&\left(\epsilon\,\partial_{tt}\boldsymbol{A}(t), \boldsymbol{v} - \partial_t\boldsymbol{A}(t)\right) + a\left(\boldsymbol{A}(t), \boldsymbol{v} - \partial_t\boldsymbol{A}(t)\right) + \varphi\left(t,\boldsymbol{v}\right) - \varphi\left(t,\partial_t\boldsymbol{A}(t)\right) \geq \left(\boldsymbol{\ell}(t), \boldsymbol{v} - \partial_t\boldsymbol{A}(t)\right),\\
&\qquad\qquad \text{for a.e. } t \in (0,T), \quad \forall\,\boldsymbol{v} \in \boldsymbol{H}_0(\mathbf{curl}\,,\Omega),\\
&\qquad\qquad \partial_t\boldsymbol{A}(0) = \tilde{\boldsymbol{E}}_0 := -\boldsymbol{E}_0, \quad \boldsymbol{A}(0) = \boldsymbol{A}_0 \quad \text{in } \Omega.
\end{aligned} \tag{9}
$$

2.3. Well-posedness of Problem 2.1

The well-posedness of problem (2) has been studied in [2, 17, 40, 42, 45, 47]. To state the result for the new formulation (9), we first make some assumptions on the material parameters, the source term, and the initial conditions.

Assumption 2.2. The following conditions hold ([41, 49]).

(H1) $\epsilon, \mu \in L^\infty(\Omega)$ are strictly positive, *i.e.*, there exist positive constants $\underline{\epsilon}, \overline{\epsilon}, \underline{\mu}, \overline{\mu} \in \mathbb{R}^+$ such that

$$\underline{\epsilon} \le \epsilon \le \overline{\epsilon}, \qquad \underline{\mu} \le \mu \le \overline{\mu}.$$

(H2) For every fixed $t \in (0,T)$, the function $j_c(\cdot,t) : \Omega \to \mathbb{R}$ is Lebesgue-measurable. Moreover, there exit two constants $C_{j_c} > 0, L_{j_c} > 0$ such that

$$0 \le j_c(\boldsymbol{x},t) \le C_{j_c},$$
$$|j_c(\boldsymbol{x},t_1) - j_c(\boldsymbol{x},t_2)| \le L_{j_c}|t_1 - t_2|,$$

for a.e. $\boldsymbol{x} \in \Omega$ and all $t, t_1, t_2 \in (0,T)$.

(H3) $\boldsymbol{\ell} \in C^{0,1}(0,T;\boldsymbol{L}^2(\Omega))$.

(H4) $\boldsymbol{E}_0 \in \boldsymbol{H}_0(\mathbf{curl}\,,\Omega)$ and $\mu^{-1}\boldsymbol{B}_0 \in \boldsymbol{X}(\Omega) \coloneqq \{\boldsymbol{q} \in \boldsymbol{H}(\mathbf{curl}\,,\Omega) : (\mu\boldsymbol{q}, \nabla\phi) = 0 \;\; \forall \phi \in H^1(\Omega)\}$.

We remark that Assumption 2.2 is reasonable in practical applications. In fact, (H1) is satisfied by general real-world materials. (H2) represents the global boundness and the Lipschitz continuity of j_c (cf. [41, 49] for more details). (H3) is only concerned with the temporal smoothness of the source and not restrictive. As given in [17, 45, 49], (H4) standards for the assumption on the initial values for the well-posedness of the $\boldsymbol{E}$-$\boldsymbol{B}$ type Maxwell variational inequality (*e.g.* (2)). Furthermore, from (H4) and (4), the initial values of (6) can be fixed, *i.e.*, $\boldsymbol{E}_0, \boldsymbol{A}_0 \in \boldsymbol{H}_0(\mathbf{curl}\,,\Omega)$.

Theorem 2.3. *Under Assumption 2.2, Problem 2.1 has a unique solution* $\boldsymbol{A} \in W^{2,\infty}(0,T;\boldsymbol{L}^2(\Omega)) \cap W^{1,\infty}(0,T;\boldsymbol{H}_0(\mathbf{curl}\,,\Omega))$ *which satisfies*

$$\|\partial_t \boldsymbol{A}\|_{L^2(0,T;\boldsymbol{L}^2_\epsilon(\Omega))} + \|\mathbf{curl}\,\boldsymbol{A}\|_{L^2(0,T;\boldsymbol{L}^2_{1/\mu}(\Omega))} \lesssim \|\boldsymbol{E}_0\|_{0,\epsilon} + \|\mathbf{curl}\,\boldsymbol{A}_0\|_{0,1/\mu} + \|\boldsymbol{\ell}\|_{L^2(0,T;\boldsymbol{L}^2(\Omega))} + \|j_c\|_{L^2(0,T;L^\infty(\Omega))}.$$

Proof. We divide the proof into three steps.

Step I. Existence of a solution $\boldsymbol{A}$. Thanks to Theorem 3.5 of [17] or Theorem 5.1 of [49], with Assumption 2.2, the Maxwell system (1) admits a unique solution $(\boldsymbol{E}, \mu^{-1}\boldsymbol{B}) \in \big(W^{1,\infty}(0,T;\boldsymbol{L}^2(\Omega)) \cap L^\infty(0,T;\boldsymbol{H}_0(\mathbf{curl}\,,\Omega))\big) \times \big(W^{1,\infty}(0,T;\boldsymbol{L}^2(\Omega)) \cap L^\infty(0,T;\boldsymbol{X}(\Omega))\big)$. By (3) and (5), we know that Problem 2.1 has at least one solution which satisfies

$$\boldsymbol{A} \in W^{2,\infty}\left(0,T;\boldsymbol{L}^2(\Omega)\right) \cap W^{1,\infty}\left(0,T;\boldsymbol{H}_0\left(\mathbf{curl}\,,\Omega\right)\right).$$

Step II. Uniqueness of the solution $\boldsymbol{A}$. Let $\boldsymbol{A}_1$ and $\boldsymbol{A}_2$ be two possible solutions of Problem 2.1. If we take $\boldsymbol{v} = \partial_t \boldsymbol{A}_2$ in the inequality (9) (resp. the analogous inequality with respect to $\boldsymbol{A}_2$), and then add the two inequalities, it follows by setting $\boldsymbol{W} = \boldsymbol{A}_1 - \boldsymbol{A}_2$ that

$$(\epsilon\,\partial_{tt}\boldsymbol{W}, \partial_t \boldsymbol{W}) + a\left(\boldsymbol{W}, \partial_t\boldsymbol{W}\right) \le 0,$$

which is equivalent to

$$\frac{\mathrm{d}}{\mathrm{d}t}\left\{\|\partial_t \boldsymbol{W}\|^2_{0,\epsilon} + a\left(\boldsymbol{W},\boldsymbol{W}\right)\right\} \le 0.$$

Since $\boldsymbol{W}(0) = 0$ and $\partial_t \boldsymbol{W}(0) = 0$ that

$$\|\partial_t \boldsymbol{W}\|^2_{0,\epsilon} + a\left(\boldsymbol{W},\boldsymbol{W}\right) = 0,$$

which shows that $\boldsymbol{W} = 0$, *i.e.*, $\boldsymbol{A}_1 = \boldsymbol{A}_2$.

Step III. Stability. Taking $\boldsymbol{v} = \mathbf{0}, 2\partial_t \boldsymbol{A}$ in (9), respectively, we obtain

$$\frac{\mathrm{d}}{\mathrm{d}t} \|\partial_t \boldsymbol{A}\|_{0,\epsilon}^2 + \frac{\mathrm{d}}{\mathrm{d}t} \|\mathbf{curl}\, \boldsymbol{A}\|_{0,1/\mu}^2 = 2\left((\boldsymbol{\ell}, \partial_t \boldsymbol{A}) - \varphi\left(t, \partial_t \boldsymbol{A}\right)\right) \leq C\left(\|\boldsymbol{\ell}\|_0 + \|j_c\|_\infty\right) \|\partial_t \boldsymbol{A}\|_{0,\epsilon}.$$

Integrating this inequality over the time interval $(0,T)$ for a fixed $t \in (0,T)$ yields

$$\|\partial_t \boldsymbol{A}\|_{0,\epsilon}^2 + \|\mathbf{curl}\, \boldsymbol{A}\|_{0,1/\mu}^2 \leq \|\partial_t \boldsymbol{A}(0)\|_{0,\epsilon}^2 + \|\mathbf{curl}\, \boldsymbol{A}(0)\|_{0,1/\mu}^2 + C\int_0^t \left(\|\boldsymbol{\ell}\|_0^2 + \|j_c\|_\infty^2\right) \mathrm{d}s + \int_0^t \|\partial_t \boldsymbol{A}\|_{0,\epsilon}^2 \,\mathrm{d}s.$$

Applying Gronwall's inequality yields the desired stability (cf. [10]). The proof is finished.

□

Remark 2.4. The threshold function j_c has three common-used forms

$$j_c(\boldsymbol{x}, t) = \begin{cases} j_c(\boldsymbol{x}, t) & \text{case 1,} \\ j_c(\boldsymbol{x}, t; \theta(\boldsymbol{x}, t)) & \text{case 2,} \\ j_c(\boldsymbol{x}, t; \theta(\boldsymbol{x}, t), \boldsymbol{B}(\boldsymbol{x}, t)) & \text{case 3,} \end{cases}$$

where $\theta(\boldsymbol{x}, t)$ stands for the temperature. We only focus on case 1 in this work.

Remark 2.5. The Ohm's law gives $\boldsymbol{J} = \sigma \boldsymbol{E}$. The conductivity $\sigma > 0$ refers to conductors, $\sigma = 0$ to dielectric materials, and $\sigma = \infty$ to perfect conductors.

3. Spatially semi-discrete approximation

Let $\mathcal{T}_h$ be a quasi-uniform partition of Ω into shape-regular tetrahedra, namely, $\overline{\Omega} = \bigcup_{K \in \mathcal{T}_h} K$. Here $h = \max_{K \in \mathcal{T}_h} h_K$ and h_K denotes the diameter of tetrahedron K. The first-order Nédélec edge element space of the second kind is defined by

$$\boldsymbol{V}_h := \left\{\boldsymbol{v}^h \in \boldsymbol{H}_0(\mathbf{curl}\,, \Omega) : \boldsymbol{v}^h|_K \in \left(\mathcal{P}_1(K)\right)^3 \;\; \forall\, K \in \mathcal{T}_h\right\},$$

where $\mathcal{P}_m(K)$ denotes the space of polynomials of degree $\leq m$ on K. The semi-discrete approximation to Problem 2.1 is given as follows:

Problem 3.1. Find $\boldsymbol{A}^h \in W^{2,\infty}(0,T; \boldsymbol{V}_h)$ such that

$$\begin{aligned} \left(\epsilon\, \partial_{tt} \boldsymbol{A}^h(t), \boldsymbol{v}^h - \partial_t \boldsymbol{A}^h(t)\right) + a\left(\boldsymbol{A}^h(t), \boldsymbol{v}^h - \partial_t \boldsymbol{A}^h(t)\right) + \varphi\left(t, \boldsymbol{v}^h\right) - \varphi\left(t, \partial_t \boldsymbol{A}^h(t)\right) \\ \geq \left(\boldsymbol{\ell}(t), \boldsymbol{v}^h - \partial_t \boldsymbol{A}^h(t)\right) \quad \text{for a.e. } t \in (0,T), \qquad \forall\, \boldsymbol{v}^h \in \boldsymbol{V}_h. \end{aligned} \tag{10}$$

We then have the following result.

Theorem 3.2. *Let Assumption 2.2 holds, Problem 3.1 has a unique solution $\boldsymbol{A}^h \in W^{2,\infty}(0,T; \boldsymbol{V}_h)$ satisfying*

$$\left\|\partial_t \boldsymbol{A}^h\right\|_{L^2(0,T; \boldsymbol{L}_\epsilon^2(\Omega))} + \left\|\mathbf{curl}\, \boldsymbol{A}^h\right\|_{L^2(0,T; \boldsymbol{L}_{1/\mu}^2(\Omega))} \leq \tilde{C},$$

where $\tilde{C} = C(\boldsymbol{E}_0, \boldsymbol{A}_0, \boldsymbol{\ell}, J_c)$.

Proof. We consider the following mixed formulation of the variational inequality, find $(\tilde{\boldsymbol{E}}^h, \tilde{\boldsymbol{B}}^h) \in W^{1,\infty}(0,T;\boldsymbol{V}_h) \times W^{1,\infty}(0,T;\boldsymbol{W}_h)$ such that

$$\begin{aligned}
&\int_\Omega \epsilon\, \partial_t \tilde{\boldsymbol{E}}^h(t) \cdot \left(\boldsymbol{v}^h - \tilde{\boldsymbol{E}}^h(t)\right) + \mu^{-1} \partial_t \tilde{\boldsymbol{B}}^h(t) \cdot \left(\boldsymbol{w}^h - \tilde{\boldsymbol{B}}^h(t)\right) \mathrm{d}\boldsymbol{x} \\
&\quad + \int_\Omega \mu^{-1} \left(\mathbf{curl}\, \tilde{\boldsymbol{E}}^h(t) \cdot \left(\boldsymbol{w}^h - \tilde{\boldsymbol{B}}^h(t)\right) - \tilde{\boldsymbol{B}}^h(t) \cdot \mathbf{curl}\left(\boldsymbol{v}^h - \tilde{\boldsymbol{E}}^h(t)\right)\right) \mathrm{d}\boldsymbol{x} + \varphi\left(t, \boldsymbol{v}^h\right) - \varphi\left(t, \tilde{\boldsymbol{E}}^h(t)\right) \\
&\quad \geq \left(\boldsymbol{\ell}(t), \boldsymbol{v}^h - \tilde{\boldsymbol{E}}^h(t)\right) \quad \text{for a.e. } t \in (0,T), \quad \forall \boldsymbol{v}^h \in \boldsymbol{V}_h, \boldsymbol{w}^h \in \boldsymbol{W}_h,
\end{aligned} \tag{11}$$

where $\boldsymbol{W}_h \subset \boldsymbol{L}^2(\Omega)$ is a family of finite-dimensional subspaces and $\mathbf{curl}\,\boldsymbol{V}_h \subset \boldsymbol{W}_h$. From the discussion in Section 4 of [45] and a classical result ([1], Thm. 4.1), we know that (11) has a unique solution $(\tilde{\boldsymbol{E}}^h, \tilde{\boldsymbol{B}}^h) \in W^{1,\infty}(0,T;\boldsymbol{V}_h) \times W^{1,\infty}(0,T;\boldsymbol{W}_h)$. Moreover, it satisfies

$$\partial_t \tilde{\boldsymbol{B}}^h + \mathbf{curl}\, \tilde{\boldsymbol{E}}^h = 0. \tag{12}$$

Set

$$\boldsymbol{A}^h(t) = \boldsymbol{A}_0^h + \int_0^t \tilde{\boldsymbol{E}}^h(s)\,\mathrm{d}s \quad \forall t \in (0,T), \tag{13}$$

with $\boldsymbol{A}_0^h \in \boldsymbol{V}_h$ satisfying $-\mathbf{curl}\,\boldsymbol{A}_0^h = \tilde{\boldsymbol{B}}_0^h$. Then by the regularity of $\tilde{\boldsymbol{E}}^h$, the construction (13) immediately yields that

$$\boldsymbol{A}^h \in W^{2,\infty}\left(0,T;\boldsymbol{V}_h\right), \quad \partial_t \boldsymbol{A}^h = \tilde{\boldsymbol{E}}^h.$$

Applying the rotational operator to (13) and using (12), we obtain

$$\mathbf{curl}\,\boldsymbol{A}^h(t) = \mathbf{curl}\,\boldsymbol{A}_0^h + \int_0^t \mathbf{curl}\,\tilde{\boldsymbol{E}}^h(s)\,\mathrm{d}s = -\tilde{\boldsymbol{B}}_0^h - \int_0^t \partial_t \tilde{\boldsymbol{B}}^h(s)\,\mathrm{d}s = -\tilde{\boldsymbol{B}}^h(t) \quad \forall t \in (0,T).$$

Now we see that $\boldsymbol{A}^h \in W^{2,\infty}(0,T;\boldsymbol{V}_h)$ satisfies (10), *i.e.*, $\boldsymbol{A}^h$ is a solution of Problem 3.1.

The arguments of uniqueness and stability of $\boldsymbol{A}^h$ are similar with Steps II and III in the proof of Theorem 2.3, we will not further elaborate here. $\square$

Let $\mathcal{I}_h$ be the canonical Nédélec edge element interpolation operator of the second kind onto $\boldsymbol{V}_h$, see [37] for its specific definition. Then there exist two positive constants C_1, C_2 independent of h such that

$$\|\boldsymbol{u} - \mathcal{I}_h \boldsymbol{u}\|_0 \leq C_1 h^2 \|\boldsymbol{u}\|_{\boldsymbol{H}^2(\Omega)} \qquad \forall \boldsymbol{u} \in \boldsymbol{H}^2(\Omega), \tag{14}$$

$$\|\mathbf{curl}\,(\boldsymbol{u} - \mathcal{I}_h \boldsymbol{u})\|_0 \leq C_2 h \|\boldsymbol{u}\|_{\boldsymbol{H}^1(\mathbf{curl},\Omega)} \quad \forall \boldsymbol{u} \in \boldsymbol{H}^1(\mathbf{curl},\Omega). \tag{15}$$

Theorem 3.3. *Let $\boldsymbol{A}(t)$ and $\boldsymbol{A}^h(t)$ be the solutions to Problems 2.1 and 3.1, respectively. Suppose the initial values $\boldsymbol{A}_0, \tilde{\boldsymbol{E}}_0 \in \boldsymbol{H}^1(\mathbf{curl},\Omega)$ and there exist finite element approximations $\boldsymbol{A}_0^h := \boldsymbol{A}^h(0), \tilde{\boldsymbol{E}}_0^h := \tilde{\boldsymbol{E}}^h(0) \in \boldsymbol{V}_h$ to $\boldsymbol{A}_0$ and $\tilde{\boldsymbol{E}}_0$, respectively, which admit the error estimates*

$$\left\|\tilde{\boldsymbol{E}}_0 - \tilde{\boldsymbol{E}}_0^h\right\|_{0,\epsilon} + \left\|\mathbf{curl}\left(\boldsymbol{A}_0 - \boldsymbol{A}_0^h\right)\right\|_{0,1/\mu} \lesssim h. \tag{16}$$

If the exact solution $\boldsymbol{A} \in W^{2,\infty}(0,T;\boldsymbol{H}^2(\Omega) \cap H^1(\mathbf{curl},\Omega))$, then

$$\left\|\partial_t \boldsymbol{A} - \partial_t \boldsymbol{A}^h\right\|_{0,\epsilon} + \left\|\mathbf{curl}\left(\boldsymbol{A} - \boldsymbol{A}^h\right)\right\|_{0,1/\mu} \lesssim h, \quad \text{for a.e. } t \in (0,T).$$

Proof. Write $\boldsymbol{e} = \boldsymbol{A} - \boldsymbol{A}^h$. It is obvious that

$$\begin{aligned}\frac{1}{2}\frac{\mathrm{d}}{\mathrm{d}t}\left[\|\dot{\boldsymbol{e}}\|_{0,\epsilon}^2 + a\left(\boldsymbol{e},\boldsymbol{e}\right)\right] &= \left(\epsilon\,\ddot{\boldsymbol{e}},\dot{\boldsymbol{e}}\right) + a\left(\boldsymbol{A}-\boldsymbol{A}^h,\partial_t\boldsymbol{A}-\partial_t\boldsymbol{A}^h\right)\\ &= \left(\epsilon\,\ddot{\boldsymbol{e}},\dot{\boldsymbol{e}}\right) + a\left(\boldsymbol{A},\partial_t\boldsymbol{A}-\partial_t\boldsymbol{A}^h\right) - a\left(\boldsymbol{A}^h,\partial_t\boldsymbol{A}-\boldsymbol{v}^h\right)\\ &\quad + a\left(\boldsymbol{A}^h,\partial_t\boldsymbol{A}^h-\boldsymbol{v}^h\right) \qquad \forall\,\boldsymbol{v}^h\in\boldsymbol{V}_h. \end{aligned}\tag{17}$$

Taking $\boldsymbol{v} = \partial_t\boldsymbol{A}^h$ in (9), we find that

$$a\left(\boldsymbol{A},\partial_t\boldsymbol{A}-\partial_t\boldsymbol{A}^h\right) \le \left(\epsilon\,\partial_{tt}\boldsymbol{A},\partial_t\boldsymbol{A}^h-\partial_t\boldsymbol{A}\right) + \varphi\left(t,\partial_t\boldsymbol{A}^h\right) - \varphi\left(t,\partial_t\boldsymbol{A}\right) - \left(\boldsymbol{\ell},\partial_t\boldsymbol{A}^h-\partial_t\boldsymbol{A}\right).\tag{18}$$

Moreover, in view of (10), we also have

$$a\left(\boldsymbol{A}^h,\partial_t\boldsymbol{A}^h-\boldsymbol{v}^h\right) \le \left(\epsilon\,\partial_{tt}\boldsymbol{A}^h,\boldsymbol{v}^h-\partial_t\boldsymbol{A}^h\right) + \varphi\left(t,\boldsymbol{v}^h\right) - \varphi\left(t,\partial_t\boldsymbol{A}^h\right) - \left(\boldsymbol{\ell},\boldsymbol{v}^h-\partial_t\boldsymbol{A}^h\right).\tag{19}$$

Using $-a(\boldsymbol{A}^h,\partial_t\boldsymbol{A}-\boldsymbol{v}^h) = a(\boldsymbol{A}-\boldsymbol{A}^h,\partial_t\boldsymbol{A}-\boldsymbol{v}^h) + a(\boldsymbol{A},\boldsymbol{v}^h-\partial_t\boldsymbol{A})$ and taking $\boldsymbol{v} = 2\partial_t\boldsymbol{A}-\boldsymbol{v}^h$ in (9), we have

$$a\left(\boldsymbol{A},\boldsymbol{v}^h-\partial_t\boldsymbol{A}\right) \le \left(\epsilon\,\partial_{tt}\boldsymbol{A},\partial_t\boldsymbol{A}-\boldsymbol{v}^h\right) + \varphi\left(t,2\partial_t\boldsymbol{A}-\boldsymbol{v}^h\right) - \varphi\left(t,\partial_t\boldsymbol{A}\right) - \left(\boldsymbol{\ell},\partial_t\boldsymbol{A}-\boldsymbol{v}^h\right).\tag{20}$$

Combining these inequalities with (17), we arrive at

$$\frac{1}{2}\frac{\mathrm{d}}{\mathrm{d}t}\left[\|\dot{\boldsymbol{e}}\|_{0,\epsilon}^2 + a\left(\boldsymbol{e},\boldsymbol{e}\right)\right] \le a\left(\boldsymbol{A}-\boldsymbol{A}^h,\partial_t\boldsymbol{A}-\boldsymbol{v}^h\right) + \left(\epsilon\,\ddot{\boldsymbol{e}},\partial_t\boldsymbol{A}-\boldsymbol{v}^h\right) + I_\varphi,\tag{21}$$

where

$$\begin{aligned} I_\varphi &= \varphi\left(t,2\partial_t\boldsymbol{A}-\boldsymbol{v}^h\right) + \varphi\left(t,\boldsymbol{v}^h\right) - 2\varphi\left(t,\partial_t\boldsymbol{A}\right)\\ &= \int_\Omega j_c(\boldsymbol{x},t)\cdot\left(\left|2\partial_t\boldsymbol{A}-\boldsymbol{v}^h\right| + \left|\boldsymbol{v}^h\right| - \left|\partial_t\boldsymbol{A}\right|\right)\,\mathrm{d}\boldsymbol{x} \le C\left\|\partial_t\boldsymbol{A}-\boldsymbol{v}^h\right\|_0.\end{aligned}\tag{22}$$

Now we integrate (21) over $(0,t)$ and use (22). This yields

$$\begin{aligned}\|\dot{\boldsymbol{e}}\|_{0,\epsilon}^2 + a\left(\boldsymbol{e},\boldsymbol{e}\right) &\lesssim \|\dot{\boldsymbol{e}}(0)\|_{0,\epsilon}^2 + \|\mathbf{curl}\,\boldsymbol{e}(0)\|_{0,1/\mu}^2 + \int_0^t\left[\left\|\mathbf{curl}\,\left(\boldsymbol{A}-\boldsymbol{A}^h\right)\right\|_{0,1/\mu}^2 + \left\|\mathbf{curl}\,\left(\partial_t\boldsymbol{A}-\boldsymbol{v}^h\right)\right\|_{0,1/\mu}^2\right]\mathrm{d}s\\ &\quad + C\int_0^t\left\|\partial_t\boldsymbol{A}-\boldsymbol{v}^h\right\|_0\,\mathrm{d}s + \int_0^t\left(\epsilon\,\ddot{\boldsymbol{e}},\partial_t\boldsymbol{A}-\boldsymbol{v}^h\right)\,\mathrm{d}s.\end{aligned}\tag{23}$$

Take $\boldsymbol{v}^h = \mathcal{I}_h\partial_t\boldsymbol{A}$ in (23) and write $\boldsymbol{d}^h = \boldsymbol{A}-\mathcal{I}_h\boldsymbol{A}$. The formula of integration by parts implies

$$\begin{aligned}\int_0^t\left(\epsilon\,\ddot{\boldsymbol{e}},\partial_t\boldsymbol{d}^h\right)\,\mathrm{d}s &= -\int_0^t\left(\epsilon\,\dot{\boldsymbol{e}},\partial_{tt}\boldsymbol{d}^h\right)\,\mathrm{d}s + \left(\epsilon\,\dot{\boldsymbol{e}},\partial_t\boldsymbol{d}^h\right)\Big|_{s=0}^{s=t}\\ &\lesssim \frac{1}{2}\int_0^t\left(\|\dot{\boldsymbol{e}}\|_{0,\epsilon}^2 + \left\|\partial_{tt}\boldsymbol{d}^h\right\|_{0,\epsilon}^2\right)\,\mathrm{d}s + \frac{\varepsilon}{2}\|\dot{\boldsymbol{e}}\|_{0,\epsilon}^2 + \frac{1}{2\varepsilon}\left\|\partial_t\boldsymbol{d}^h\right\|_{0,\epsilon}^2 + \frac{1}{2}\|\dot{\boldsymbol{e}}(0)\|_{0,\epsilon}^2 + \frac{1}{2}\left\|\partial_t\boldsymbol{d}^h(0)\right\|_{0,\epsilon}^2.\end{aligned}$$

Inserting the above inequality into (23) and using Gronwall's inequality, we arrive at

$$\begin{aligned}\|\dot{\boldsymbol{e}}\|_{0,\epsilon} + \|\mathbf{curl}\,\boldsymbol{e}\|_{0,1/\mu} &\lesssim \|\dot{\boldsymbol{e}}(0)\|_{0,\epsilon} + \|\mathbf{curl}\,\boldsymbol{e}(0)\|_{0,1/\mu} + \left\|\mathbf{curl}\,\partial_t\boldsymbol{d}^h\right\|_{L^2(0,T;\boldsymbol{L}^2(\Omega))} + \left\|\partial_t\boldsymbol{d}^h\right\|_{L^2(0,T;\boldsymbol{L}^2(\Omega))}^{1/2}\\ &\quad + \left\|\partial_{tt}\boldsymbol{d}^h\right\|_{L^2(0,T;\boldsymbol{L}_\epsilon^2(\Omega))} + \left\|\partial_t\boldsymbol{d}^h\right\|_{0,\epsilon} + \left\|\partial_t\boldsymbol{d}^h(0)\right\|_{0,\epsilon}.\end{aligned}$$

Using (14), (15) and inequality (16), we obtain $\left\|\dot{\boldsymbol{e}}\right\|_{0,\epsilon} + \left\|\mathbf{curl}\,\boldsymbol{e}\right\|_{0,1/\mu} \lesssim h$. The proof is finished. $\square$

4. A fully discrete scheme

Let $N > 0$ be a positive integer and $\tau = T/N$ be the time-step size. A partition of the time interval $[0, T]$ is given by $t_k = k\tau$, $k = 0, 1, \cdots, N$. Define the time-difference operators

$$\delta_{tt}\boldsymbol{A}_k = \frac{\boldsymbol{A}_k - 2\boldsymbol{A}_{k-1} + \boldsymbol{A}_{k-2}}{\tau^2}, \qquad \delta_t\boldsymbol{A}_k = \frac{\boldsymbol{A}_k - \boldsymbol{A}_{k-1}}{\tau}, \qquad k \geq 1.$$

For convenience, we shall also use the notations $\tilde{\boldsymbol{E}}_k := \delta_t\boldsymbol{A}_k (k \geq 0)$ and $\boldsymbol{A}_{-1} := \boldsymbol{A}_0 - \tau\tilde{\boldsymbol{E}}_0$. In fact, $-\delta_t\boldsymbol{A}_k$ is the approximation of $\boldsymbol{E}$ due to its definition (3).

4.1. Fully discrete scheme

A first-order fully discrete scheme is designed based on the backward time-difference scheme and first-order finite element discretization for Problem 2.1.

Problem 4.1. Find $\{\boldsymbol{A}_k^h\}_{k=1}^N \subset \boldsymbol{V}_h$ such that

$$\left(\epsilon\,\delta_{tt}\boldsymbol{A}_k^h, \boldsymbol{v}^h - \delta_t\boldsymbol{A}_k^h\right) + a\left(\boldsymbol{A}_k^h, \boldsymbol{v}^h - \delta_t\boldsymbol{A}_k^h\right) + \varphi\left(t_k, \boldsymbol{v}^h\right) - \varphi\left(t_k, \delta_t\boldsymbol{A}_k^h\right) \geq \left(\boldsymbol{\ell}_k, \boldsymbol{v}^h - \delta_t\boldsymbol{A}_k^h\right) \quad \forall\, \boldsymbol{v}^h \in \boldsymbol{V}_h, \tag{24}$$

where the initial values and the right-hand side are defined by

$$\boldsymbol{A}_0^h = \mathcal{I}_h\boldsymbol{A}_0, \quad \tilde{\boldsymbol{E}}_0^h = \mathcal{I}_h\tilde{\boldsymbol{E}}_0, \quad \boldsymbol{\ell}_k = \frac{1}{\tau}\int_{t_{k-1}}^{t_k}\boldsymbol{\ell}(t)\,\mathrm{d}t, \tag{25}$$

and the discrete approximations $\boldsymbol{A}_0^h$, $\tilde{\boldsymbol{E}}_0^h$ satisfy (16).

Using the definition $\tilde{\boldsymbol{E}}_k^h = \delta_t\boldsymbol{A}_k^h$, we can formulate (24) into an equivalent form.

Problem 4.2. Find $\{\tilde{\boldsymbol{E}}_k^h\}_{k=1}^N \subset \boldsymbol{V}_h$ such that

$$\tilde{a}\left(\tilde{\boldsymbol{E}}_k^h, \boldsymbol{v}^h - \tilde{\boldsymbol{E}}_k^h\right) + \varphi\left(t_k, \boldsymbol{v}^h\right) - \varphi\left(t_k, \tilde{\boldsymbol{E}}_k^h\right) \geq \left(\boldsymbol{f}_k^h, \boldsymbol{v}^h - \tilde{\boldsymbol{E}}_k^h\right) \qquad \forall\, \boldsymbol{v}^h \in \boldsymbol{V}_h, \tag{26}$$

where the bilinear form $\tilde{a} : \boldsymbol{V}_h \times \boldsymbol{V}_h \to \mathbb{R}$ and the linear form $\boldsymbol{f}_k^h : \boldsymbol{V}_h \to \mathbb{R}$ are, respectively, defined by

$$\tilde{a}\left(\boldsymbol{v}^h, \boldsymbol{w}^h\right) = \tau^{-1}\left(\epsilon\,\boldsymbol{v}^h, \boldsymbol{w}^h\right) + \tau a\left(\boldsymbol{v}^h, \boldsymbol{w}^h\right), \qquad \left(\boldsymbol{f}_k^h, \boldsymbol{v}^h\right) = \left(\tau^{-1}\epsilon\tilde{\boldsymbol{E}}_{k-1}^h - \boldsymbol{\ell}_k, \boldsymbol{v}^h\right) + a\left(\boldsymbol{A}_{k-1}^h, \boldsymbol{v}^h\right).$$

By the classical theory in [30], Problem 4.2 has a unique solution $\tilde{\boldsymbol{E}}_k^h \in \boldsymbol{V}_h$ for each $k \geq 1$. The following theorem gives the stability of the numerical solutions.

Theorem 4.3. *Suppose $\boldsymbol{\ell}_k^{(j)} \in L^2(0, T; \boldsymbol{L}^2(\Omega))$ and $\{\boldsymbol{A}_k^{(j),h}\}$ are the numerical solutions of Problem 4.1 corresponding to $\boldsymbol{\ell}_k^{(j)}$ for $j = 1, 2$ with the initial values $\boldsymbol{A}_0^{(1),h} = \boldsymbol{A}_0^{(2),h}$ and $\tilde{\boldsymbol{E}}_0^{(1),h} = \tilde{\boldsymbol{E}}_0^{(2),h}$. Then the stability of Lipschitz continuity holds*

$$\left\|\delta_t\boldsymbol{A}_k^{(1),h} - \delta_t\boldsymbol{A}_k^{(2),h}\right\|_{0,\epsilon} + \left\|\mathbf{curl}\,\boldsymbol{A}_k^{(1),h} - \mathbf{curl}\,\boldsymbol{A}_k^{(2),h}\right\|_{0,1/\mu} \lesssim \left\|\boldsymbol{\ell}_k^{(1)} - \boldsymbol{\ell}_k^{(2)}\right\|_{L^2(0,T;\boldsymbol{L}^2(\Omega))}. \tag{27}$$

Moreover, if $\boldsymbol{\ell}$ satisfies (H3), the numerical solutions satisfy

$$\max_{k=0,\cdots,N}\left(\left\|\boldsymbol{A}_k^h\right\|_{0,\epsilon} + \left\|\mathbf{curl}\,\boldsymbol{A}_k^h\right\|_{0,1/\mu} + \left\|\delta_t\tilde{\boldsymbol{E}}_k^h\right\|_{0,\epsilon} + \left\|\mathbf{curl}\,\tilde{\boldsymbol{E}}_k^h\right\|_{0,1/\mu}\right) \leq C. \tag{28}$$

Proof. First we prove the stability of Lipschitz continuity. From (24), we have, for any $\boldsymbol{v}^h \in \boldsymbol{V}_h$,

$$\begin{aligned}\left(\epsilon\,\delta_t \tilde{\boldsymbol{E}}_k^{(j),h}, \boldsymbol{v}^h - \tilde{\boldsymbol{E}}_k^{(j),h}\right) + a\left(\boldsymbol{A}_k^{(j),h}, \boldsymbol{v}^h - \tilde{\boldsymbol{E}}_k^{(j),h}\right) + \varphi\left(t_k, \boldsymbol{v}^h\right) - \varphi\left(t_k, \tilde{\boldsymbol{E}}_k^{(j),h}\right)&\\ \geq \left(\boldsymbol{\ell}_k^{(j)}, \boldsymbol{v}^h - \tilde{\boldsymbol{E}}_k^{(j),h}\right) \quad j = 1, 2.&\end{aligned} \tag{29}$$

Taking $\boldsymbol{v}^h = \tilde{\boldsymbol{E}}_k^{(2),h}$ for $j = 1$ and $\boldsymbol{v}^h = \tilde{\boldsymbol{E}}_k^{(1),h}$ for $j = 2$ in (29), we obtain

$$\begin{aligned}\left(\epsilon\,\delta_t \tilde{\boldsymbol{E}}_k^{(1),h}, \tilde{\boldsymbol{E}}_k^{(1),h} - \tilde{\boldsymbol{E}}_k^{(2),h}\right) + a\left(\boldsymbol{A}_k^{(1),h}, \tilde{\boldsymbol{E}}_k^{(1),h} - \tilde{\boldsymbol{E}}_k^{(2),h}\right) - \varphi\left(t_k, \tilde{\boldsymbol{E}}_k^{(2),h}\right) + \varphi\left(t_k, \tilde{\boldsymbol{E}}_k^{(1),h}\right)&\\ \leq \left(\boldsymbol{\ell}_k^{(1)}, \tilde{\boldsymbol{E}}_k^{(1),h} - \tilde{\boldsymbol{E}}_k^{(2),h}\right),&\\ \left(-\epsilon\,\delta_t \tilde{\boldsymbol{E}}_k^{(2),h}, \tilde{\boldsymbol{E}}_k^{(1),h} - \tilde{\boldsymbol{E}}_k^{(2),h}\right) + a\left(-\boldsymbol{A}_k^{(2),h}, \tilde{\boldsymbol{E}}_k^{(1),h} - \tilde{\boldsymbol{E}}_k^{(2),h}\right) + \varphi\left(t_k, \tilde{\boldsymbol{E}}_k^{(2),h}\right) - \varphi\left(t_k, \tilde{\boldsymbol{E}}_k^{(1),h}\right)&\\ \leq \left(-\boldsymbol{\ell}_k^{(2)}, \tilde{\boldsymbol{E}}_k^{(1),h} - \tilde{\boldsymbol{E}}_k^{(2),h}\right).&\end{aligned}$$

Adding the above two inequalities yields

$$\left(\epsilon\,\delta_t \boldsymbol{\xi}_k^h, \boldsymbol{\xi}_k^h\right) + a\left(\boldsymbol{\zeta}_k^h, \delta_t \boldsymbol{\zeta}_k^h\right) \leq \left(\boldsymbol{\ell}_k^{(1)} - \boldsymbol{\ell}_k^{(2)}, \boldsymbol{\xi}_k^h\right), \tag{30}$$

where $\boldsymbol{\zeta}_k^h := \boldsymbol{A}_k^{(1),h} - \boldsymbol{A}_k^{(2),h}$ and $\boldsymbol{\xi}_k^h := \delta_t \boldsymbol{\zeta}_k^h = \tilde{\boldsymbol{E}}_k^{(1),h} - \tilde{\boldsymbol{E}}_k^{(2),h}$.

Now using the identity $2x(x-y) = x^2 - y^2 + (x-y)^2$, we deduce that

$$\begin{aligned}2\left(\epsilon\,\delta_t \boldsymbol{\xi}_k^h, \boldsymbol{\xi}_k^h\right) &= \tau^{-1}\left\|\boldsymbol{\xi}_k^h\right\|_{0,\epsilon}^2 - \tau^{-1}\left\|\boldsymbol{\xi}_{k-1}^h\right\|_{0,\epsilon}^2 + \left\|\delta_t \boldsymbol{\xi}_k^h\right\|_{0,\epsilon}^2,\\ 2a\left(\boldsymbol{\zeta}_k^h, \delta_t \boldsymbol{\zeta}_k^h\right) &= \tau^{-1} a\left(\boldsymbol{\zeta}_k^h, \boldsymbol{\zeta}_k^h\right) - \tau^{-1} a\left(\boldsymbol{\zeta}_{k-1}^h, \boldsymbol{\zeta}_{k-1}^h\right) + a\left(\delta_t \boldsymbol{\zeta}_k^h, \delta_t \boldsymbol{\zeta}_k^h\right).\end{aligned}$$

Substituting the two equalities into (30) and summing up the inequalities for $k = 0, \cdots, n\,(0 \leq n \leq N)$, we have

$$\left\|\boldsymbol{\xi}_n^h\right\|_{0,\epsilon}^2 + a\left(\boldsymbol{\zeta}_n^h, \boldsymbol{\zeta}_n^h\right) \lesssim \tau \sum_{k=0}^{n} \left\|\boldsymbol{\ell}_k^{(1)} - \boldsymbol{\ell}_k^{(2)}\right\|_0^2 + \tau \sum_{k=0}^{n} \left\|\boldsymbol{\xi}_k^h\right\|_{0,\epsilon}^2.$$

Since $\boldsymbol{\xi}_0^h = \mathbf{0}$, $\boldsymbol{\zeta}_0^h = \mathbf{0}$, by the assumptions, applying the discrete Gronwall's inequality yields (27).

Next we prove (28). Taking $\boldsymbol{v}_h = 0, 2\tilde{\boldsymbol{E}}_k^h$ in (24), respectively, we get

$$\frac{1}{\tau}\left(\epsilon \cdot \left(\tilde{\boldsymbol{E}}_k^h - \tilde{\boldsymbol{E}}_{k-1}^h\right), \tilde{\boldsymbol{E}}_k^h\right) + a\left(\boldsymbol{A}_k^h, \tilde{\boldsymbol{E}}_k^h\right) = \left(\boldsymbol{\ell}_k, \tilde{\boldsymbol{E}}_k^h\right) - \varphi\left(t_k, \tilde{\boldsymbol{E}}_k^h\right). \tag{31}$$

Then we see

$$\left\|\tilde{\boldsymbol{E}}_k^h\right\|_{0,\epsilon}^2 - \left\|\tilde{\boldsymbol{E}}_{k-1}^h\right\|_{0,\epsilon}^2 + \left\|\mathbf{curl}\,\boldsymbol{A}_k^h\right\|_{0,1/\mu}^2 - \left\|\mathbf{curl}\,\boldsymbol{A}_{k-1}^h\right\|_{0,1/\mu}^2 \lesssim \tau\left(\|\boldsymbol{\ell}_k\|_0 + \|j_c\|_\infty\right)\left\|\tilde{\boldsymbol{E}}_k^h\right\|_{0,\epsilon}.$$

Summing up k from 1 to $n\,(n \leq N)$, leads to

$$\left\|\tilde{\boldsymbol{E}}_n^h\right\|_{0,\epsilon}^2 + \left\|\mathbf{curl}\,\boldsymbol{A}_n^h\right\|_{0,1/\mu}^2 \lesssim \tau \sum_{k=0}^{n} \left\|\tilde{\boldsymbol{E}}_k^h\right\|_{0,\epsilon}^2 + \tau \sum_{k=0}^{n}\left(\|\boldsymbol{\ell}_k\|_0^2 + \|j_c\|_\infty^2\right) + \left\|\tilde{\boldsymbol{E}}_0^h\right\|_{0,\epsilon}^2 + \left\|\mathbf{curl}\,\boldsymbol{A}_0^h\right\|_{0,1/\mu}^2.$$

By Gronwall's inequality, we then obtain the stability

$$\left\|\tilde{\boldsymbol{E}}_n^h\right\|_{0,\epsilon}+\left\|\mathbf{curl}\ \boldsymbol{A}_n^h\right\|_{0,1/\mu}\le C,\quad 0\le n\le N.$$

$$i.e.\quad \max_{k=0,\cdots,N}\left\{\left\|\tilde{\boldsymbol{E}}_k^h\right\|_{0,\epsilon}+\left\|\mathbf{curl}\ \boldsymbol{A}_k^h\right\|_{0,1/\mu}\right\}\le C.$$

Due to the fact

$$\boldsymbol{A}_k^h=\boldsymbol{A}_0^h+\tau\sum_{i=1}^{k}\tilde{\boldsymbol{E}}_i^h,$$

we have

$$\max_{k=0,\cdots,N}\left\|\boldsymbol{A}_k^h\right\|_{0,\epsilon}\le C.$$

Besides, fixing j and discarding such superscript, taking $\boldsymbol{v}^h=\tilde{\boldsymbol{E}}_{k+1}^h$ in the kth inequality of (29) and $\boldsymbol{v}^h=\tilde{\boldsymbol{E}}_k^h$ in the $(k+1)^{\text{th}}$ inequality, we have

$$\left(-\epsilon\,\delta_t\tilde{\boldsymbol{E}}_k^h,\tilde{\boldsymbol{E}}_{k+1}^h-\tilde{\boldsymbol{E}}_k^h\right)+a\left(-\boldsymbol{A}_k^h,\tilde{\boldsymbol{E}}_{k+1}^h-\tilde{\boldsymbol{E}}_k^h\right)-\varphi\left(t_k,\tilde{\boldsymbol{E}}_{k+1}^h\right)+\varphi\left(t_k,\tilde{\boldsymbol{E}}_k^h\right)\le\left(-\boldsymbol{\ell}_k,\tilde{\boldsymbol{E}}_{k+1}^h-\tilde{\boldsymbol{E}}_k^h\right),$$
$$\left(\epsilon\,\delta_t\tilde{\boldsymbol{E}}_{k+1}^h,\tilde{\boldsymbol{E}}_{k+1}^h-\tilde{\boldsymbol{E}}_k^h\right)+a\left(\boldsymbol{A}_{k+1}^h,\tilde{\boldsymbol{E}}_{k+1}^h-\tilde{\boldsymbol{E}}_k^h\right)-\varphi\left(t_{k+1},\tilde{\boldsymbol{E}}_k^h\right)+\varphi\left(t_{k+1},\tilde{\boldsymbol{E}}_{k+1}^h\right)\le\left(\boldsymbol{\ell}_{k+1},\tilde{\boldsymbol{E}}_{k+1}^h-\tilde{\boldsymbol{E}}_k^h\right).$$

Adding the above two inequalities results in

$$\begin{aligned}&\left(\epsilon\,\delta_t\left(\tilde{\boldsymbol{E}}_{k+1}^h-\tilde{\boldsymbol{E}}_k^h\right),\delta_t\tilde{\boldsymbol{E}}_{k+1}^h\right)+a\left(\tilde{\boldsymbol{E}}_{k+1}^h,\tilde{\boldsymbol{E}}_{k+1}^h-\tilde{\boldsymbol{E}}_k^h\right)\\&\quad\le\frac{1}{\tau}\left\{\varphi\left(t_k,\tilde{\boldsymbol{E}}_{k+1}^h\right)-\varphi\left(t_k,\tilde{\boldsymbol{E}}_k^h\right)-\varphi\left(t_{k+1},\tilde{\boldsymbol{E}}_{k+1}^h\right)+\varphi\left(t_{k+1},\tilde{\boldsymbol{E}}_k^h\right)\right\}+\left(\boldsymbol{\ell}_{k+1}-\boldsymbol{\ell}_k,\delta_t\tilde{\boldsymbol{E}}_{k+1}^h\right).\end{aligned}$$

This implies

$$\begin{aligned}&\left\|\delta_t\tilde{\boldsymbol{E}}_{k+1}^h\right\|_{0,\epsilon}^2-\left\|\delta_t\tilde{\boldsymbol{E}}_k^h\right\|_{0,\epsilon}^2+\left\|\mathbf{curl}\,\tilde{\boldsymbol{E}}_{k+1}^h\right\|_{0,1/\mu}^2-\left\|\mathbf{curl}\,\tilde{\boldsymbol{E}}_k^h\right\|_{0,1/\mu}^2\\&\qquad\le\frac{1}{2}\int_\Omega\left(j_c\left(\boldsymbol{x},t_{k+1}\right)-j_c\left(\boldsymbol{x},t_k\right)\right)\cdot\frac{\left|\tilde{\boldsymbol{E}}_k^h\right|-\left|\tilde{\boldsymbol{E}}_{k+1}^h\right|}{\tau}\,\mathrm{d}\boldsymbol{x}+\frac{1}{2}\left(\boldsymbol{\ell}_{k+1}-\boldsymbol{\ell}_k,\delta_t\tilde{\boldsymbol{E}}_{k+1}^h\right)\\&\qquad\lesssim\tau\left\|\frac{j_c\left(\boldsymbol{x},t_{k+1}\right)-j_c\left(\boldsymbol{x},t_k\right)}{\tau}\right\|_0\cdot\left\|\delta_t\tilde{\boldsymbol{E}}_{k+1}^h\right\|_{0,\epsilon}+\tau\int_{t_k}^{t_{k+1}}\left(\partial_t\boldsymbol{\ell}(t),\delta_t\tilde{\boldsymbol{E}}_{k+1}^h\right)\,\mathrm{d}t.\end{aligned}$$

Summing up the above inequalities for $k=0,\cdots,n(n\le N-1)$, employing (H2) and Gronwall's inequality, we obtain

$$\left\|\delta_t\tilde{\boldsymbol{E}}_{n+1}^h\right\|_{0,\epsilon}^2+\left\|\mathbf{curl}\,\tilde{\boldsymbol{E}}_{n+1}^h\right\|_{0,1/\mu}^2\lesssim\left\|\boldsymbol{A}_0^h\right\|_{0,\epsilon}^2+\left\|\mathbf{curl}\,\tilde{\boldsymbol{E}}_0^h\right\|_{0,1/\mu}^2+L_{j_c}+\tau^2\left\|\partial_t\boldsymbol{\ell}\right\|_{\boldsymbol{L}^2(0,T;L^2(\Omega))}^2\le C.$$

The proof is finished. □

4.2. *A priori* error analysis

The objective of this subsection is to derive an error estimate for the fully discrete problem. Define $\boldsymbol{A}_k=\boldsymbol{A}(t_k)$, $\partial_t\boldsymbol{A}_k=(\partial_t\boldsymbol{A})(t_k)$, and $\partial_{tt}\boldsymbol{A}_k=(\partial_{tt}\boldsymbol{A})(t_k)$ for $0\le k\le N$. We also denote $\partial_t^2\cdot:=\partial_{tt}\cdot$ and $\delta_t^2\cdot:=\delta_t(\delta_t\cdot)$ and so forth.

Theorem 4.4. *Let $\boldsymbol{A}$ and $\boldsymbol{A}_k^h$ be the solutions of Problems 2.1 and 4.1, respectively. Suppose*

- *Assumption 2.2 holds,*
- $\boldsymbol{A} \in \boldsymbol{W}^{3,\infty}(0,T;\boldsymbol{L}^2(\Omega)) \cap \boldsymbol{W}^{2,\infty}(0,T;\boldsymbol{H}^2(\Omega)\cap \boldsymbol{H}_0(\mathbf{curl}\,,\Omega))$.

Then the following error estimate holds

$$\max_{k=0,\cdots,N}\left\{\left\|\delta_t\left(\boldsymbol{A}_k-\boldsymbol{A}_k^h\right)\right\|_{0,\epsilon}+\left\|\mathbf{curl}\,\left(\boldsymbol{A}_k-\boldsymbol{A}_k^h\right)\right\|_{0,1/\mu}\right\}\lesssim h+\tau.$$

Proof. For convenience, we define $\boldsymbol{e}_k=\boldsymbol{A}_k-\boldsymbol{A}_k^h$ and $\mathscr{A}_k=(\epsilon\,\delta_{tt}\boldsymbol{e}_k,\delta_t\boldsymbol{e}_k)+a(\boldsymbol{e}_k,\delta_t\boldsymbol{e}_k)$. It is clear that

$$2\tau\mathscr{A}_k\geq\|\delta_t\boldsymbol{e}_k\|_{0,\epsilon}^2-\|\delta_t\boldsymbol{e}_{k-1}\|_{0,\epsilon}^2+\|\mathbf{curl}\,\boldsymbol{e}_k\|_{0,1/\mu}^2-\|\mathbf{curl}\,\boldsymbol{e}_{k-1}\|_{0,1/\mu}^2. \tag{32}$$

To estimate the upper bound of $\mathscr{A}_k$, we take $\boldsymbol{v}=\delta_t\boldsymbol{A}_k^h$ in (9) at $t=t_k$. It gives

$$\left(\epsilon\,\partial_{tt}\boldsymbol{A}_k,\delta_t\boldsymbol{A}_k^h-\partial_t\boldsymbol{A}_k\right)+a\left(\boldsymbol{A}_k,\delta_t\boldsymbol{A}_k^h-\partial_t\boldsymbol{A}_k\right)\geq\left(\boldsymbol{\ell}_k,\delta_t\boldsymbol{A}_k^h-\partial_t\boldsymbol{A}_k\right)-\varphi\left(t_k,\delta_t\boldsymbol{A}_k^h\right)+\varphi\left(t_k,\partial_t\boldsymbol{A}_k\right).$$

Similarly, taking $\boldsymbol{v}^h=\mathcal{I}_h(\partial_t\boldsymbol{A}_k)$ in (24) yields

$$\begin{aligned}\left(\epsilon\,\delta_{tt}\boldsymbol{A}_k^h,\mathcal{I}_h\left(\partial_t\boldsymbol{A}_k\right)-\delta_t\boldsymbol{A}_k^h\right)+a\left(\boldsymbol{A}_k^h,\mathcal{I}_h\left(\partial_t\boldsymbol{A}_k\right)-\delta_t\boldsymbol{A}_k^h\right)\geq\left(\boldsymbol{\ell}_k,\mathcal{I}_h\left(\partial_t\boldsymbol{A}_k\right)-\delta_t\boldsymbol{A}_k^h\right)-\varphi\left(t_k,\mathcal{I}_h\left(\partial_t\boldsymbol{A}_k\right)\right)\\+\varphi\left(t_k,\delta_t\boldsymbol{A}_k^h\right).\end{aligned}$$

Write $\boldsymbol{\eta}_k:=\mathcal{I}_h(\partial_t\boldsymbol{A}_k)-\partial_t\boldsymbol{A}_k$ for convenience. Manipulating the terms of $\mathscr{A}_k$ properly and using the above two inequalities, we obtain

$$\begin{aligned}\mathscr{A}_k=&-\left(\epsilon\,\partial_{tt}\boldsymbol{A}_k,\delta_t\boldsymbol{A}_k^h-\partial_t\boldsymbol{A}_k\right)-a\left(\boldsymbol{A}_k,\delta_t\boldsymbol{A}_k^h-\partial\boldsymbol{A}_k\right)-\left(\epsilon\,\delta_{tt}\boldsymbol{A}_k^h,\mathcal{I}_h\left(\partial_t\boldsymbol{A}_k\right)-\delta_t\boldsymbol{A}_k^h\right)\\&-a\left(\boldsymbol{A}_k^h,\mathcal{I}_h\left(\partial_t\boldsymbol{A}_k\right)-\delta_t\boldsymbol{A}_k^h\right)+\underbrace{\left(\epsilon\,\left(\delta_{tt}\boldsymbol{A}_k-\partial_{tt}\boldsymbol{A}_k\right),\delta_t\boldsymbol{e}_k+\boldsymbol{\eta}_k+\partial_t\boldsymbol{A}_k-\delta_t\boldsymbol{A}_k\right)}_{R_k^{(1)}}\\&+\underbrace{\left(\epsilon\,\delta_{tt}\boldsymbol{e}_k,\delta_t\boldsymbol{A}_k-\partial_t\boldsymbol{A}_k-\boldsymbol{\eta}_k\right)}_{R_k^{(2)}}+\underbrace{a\left(\boldsymbol{e}_k,\delta_t\boldsymbol{A}_k-\partial_t\boldsymbol{A}_k-\boldsymbol{\eta}_k\right)}_{R_k^{(3)}}+\left(\epsilon\,\partial_{tt}\boldsymbol{A}_k,\boldsymbol{\eta}_k\right)+a\left(\boldsymbol{A}_k,\boldsymbol{\eta}_k\right)\\\leq\;&R_k^{(1)}+R_k^{(2)}+R_k^{(3)}+\underbrace{\varphi\left(t_k,\mathcal{I}_h\left(\partial_t\boldsymbol{A}_k\right)\right)-\varphi\left(t_k,\partial_t\boldsymbol{A}_k\right)}_{R_k^{(4)}}+\underbrace{\left(\epsilon\,\partial_{tt}\boldsymbol{A}_k,\boldsymbol{\eta}_k\right)+a\left(\boldsymbol{A}_k,\boldsymbol{\eta}_k\right)-\left(\boldsymbol{\ell}_k,\boldsymbol{\eta}_k\right)}_{R_k^{(5)}}.\end{aligned}$$

Together with (32), this shows

$$\|\delta_t\boldsymbol{e}_n\|_{0,\epsilon}^2+\|\mathbf{curl}\,\boldsymbol{e}_n\|_{0,1/\mu}^2\lesssim\sum_{k=1}^n\sum_{i=1}^5\tau R_k^{(i)}+\left\|\delta_t\boldsymbol{e}_0\right\|_{0,\epsilon}^2+\left\|\mathbf{curl}\,\boldsymbol{e}_0\right\|_{0,1/\mu}^2,\qquad 1\leq n\leq N. \tag{33}$$

In the rest of the proof, we are going to estimate each term on the right-hand side of (33).

For any smooth function f of t, Taylor's formula shows that

$$\begin{aligned}\delta_{tt}f_j&=\frac{f_j-2f_{j-1}+f_{j-2}}{\tau^2}=\partial_{tt}f_j-\frac{\tau}{2}\int_0^2\partial_t^3f(t_{j-2}+\tau s)s^2\,\mathrm{d}s+\tau\int_0^1\partial_t^3f(t_{j-1}+s\tau)s^2\,\mathrm{d}s,\\\delta_tf_j&=\frac{f_j-f_{j-1}}{\tau}=\partial_tf_j-\tau\int_0^1\partial_{tt}f(t_{j-1}+s\tau)s\,\mathrm{d}s,\\\delta_t\left(\delta_tf_j-\partial_tf_j\right)&=\frac{\delta_tf_j-\partial_tf_j}{\tau}-\frac{\delta_tf_{j-1}-\partial_tf_{j-1}}{\tau}=-\tau\int_0^1\int_0^1\partial_t^3f\left(t_{j-2}+r\tau+s\tau\right)s\,\mathrm{d}r\,\mathrm{d}s.\end{aligned}$$

They show that

$$\left\|\delta_t\left(\mathbf{curl}\,\boldsymbol{A}_k\right)-\partial_t\left(\mathbf{curl}\,\boldsymbol{A}_k\right)\right\|_{0,1/\mu}\lesssim\tau\left\|\partial_{tt}(\mathbf{curl}\,\boldsymbol{A})\right\|_{\boldsymbol{L}^\infty(t_{k-1},t_k;\boldsymbol{L}^2(\Omega))},\tag{34}$$

$$\left\|\delta_t^m\boldsymbol{A}_k-\partial_t^m\boldsymbol{A}_k\right\|_{0,\epsilon}\lesssim\tau\left\|\partial_t^{m+1}\boldsymbol{A}\right\|_{\boldsymbol{L}^\infty(t_{k-m},t_k;\boldsymbol{L}^2(\Omega))}\quad(m=1,2),\tag{35}$$

$$\left\|\delta_t\left(\delta_t\boldsymbol{A}_k-\partial_t\boldsymbol{A}_k\right)\right\|_{0,\epsilon}\lesssim\tau\left\|\partial_t^3\boldsymbol{A}\right\|_{\boldsymbol{L}^\infty(t_{k-2},t_k;\boldsymbol{L}^2(\Omega))}.\tag{36}$$

Moreover, using (14) and (15), we also have

$$\|\boldsymbol{\eta}_k\|_{0,\epsilon}\lesssim h^2\left\|\partial_t\boldsymbol{A}_k\right\|_{\boldsymbol{H}^2(\Omega)},\qquad\|\boldsymbol{\eta}_k\|_{\mathbf{curl}}\lesssim h\left\|\partial_t\boldsymbol{A}_k\right\|_{\boldsymbol{H}^1(\mathbf{curl},\Omega)}\tag{37}$$

$$\|\delta_t\boldsymbol{\eta}_k\|_{0,\epsilon}=\left\|\mathcal{I}_h\left(\delta_t\partial_t\boldsymbol{A}_k\right)-\delta_t\partial_t\boldsymbol{A}_k\right\|_{0,\epsilon}\lesssim h^2\left\|\delta_t\partial_t\boldsymbol{A}_k\right\|_{\boldsymbol{H}^2(\Omega)}\lesssim h^2\left\|\partial_{tt}\boldsymbol{A}\right\|_{\boldsymbol{L}^\infty(t_{k-1},t_k;\boldsymbol{H}^2(\Omega))}.\tag{38}$$

It follows that

$$\begin{aligned}\sum_{k=1}^n\tau R_k^{(1)}&\lesssim\tau\sum_{k=1}^n\left\|\delta_{tt}\boldsymbol{A}_k-\partial_{tt}\boldsymbol{A}_k\right\|_{0,\epsilon}\left(\|\delta_t\boldsymbol{e}_k\|_{0,\epsilon}+\|\boldsymbol{\eta}_k\|_{0,\epsilon}+\|\delta_t\boldsymbol{A}_k-\partial_t\boldsymbol{A}_k\|_{0,\epsilon}\right)\\&\lesssim\tau^2\|\boldsymbol{A}\|_{\boldsymbol{W}^{3,\infty}(0,T;\boldsymbol{L}^2(\Omega))}\sum_{k=1}^n\left(\|\delta_t\boldsymbol{e}_k\|_{0,\epsilon}+h^2\left\|\partial_t\boldsymbol{A}_k\right\|_{\boldsymbol{H}^2(\Omega)}+\tau\|\boldsymbol{A}\|_{\boldsymbol{W}^{2,\infty}(0,T;\boldsymbol{L}^2(\Omega))}\right)\\&\lesssim\tau\left(\tau+h^2\right)+\tau\left(\sum_{k=1}^n\tau\|\delta_t\boldsymbol{e}_k\|_{0,\epsilon}^2\right)^{1/2}.\end{aligned}\tag{39}$$

Similarly, using summation by parts and the inequalities (36)–(38), we get

$$\begin{aligned}\sum_{k=1}^n\tau R_k^{(2)}&=\sum_{k=1}^n\tau\left(\epsilon\,\delta_{tt}\boldsymbol{e}_k,\delta_t\boldsymbol{A}_k-\partial_t\boldsymbol{A}_k-\boldsymbol{\eta}_k\right)\\&=\left(\epsilon\,\delta_t\boldsymbol{e}_n,\delta_t\boldsymbol{A}_n-\partial_t\boldsymbol{A}_n-\boldsymbol{\eta}_n\right)-\left(\epsilon\,\delta_t\boldsymbol{e}_0,\delta_t\boldsymbol{A}_1-\partial_t\boldsymbol{A}_1-\boldsymbol{\eta}_1\right)-\sum_{k=2}^n\tau\left(\epsilon\,\delta_t\boldsymbol{e}_{k-1},\delta_t\left(\delta_t\boldsymbol{A}_k-\partial_t\boldsymbol{A}_k-\boldsymbol{\eta}_k\right)\right)\\&\lesssim\|\delta_t\boldsymbol{e}_n\|_{0,\epsilon}\left(\tau\left\|\partial_t^2\boldsymbol{A}\right\|_{\boldsymbol{L}^\infty(t_{n-1},t_n;\boldsymbol{L}^2(\Omega))}+h^2\left\|\partial_t\boldsymbol{A}_n\right\|_{\boldsymbol{H}^2(\Omega)}\right)\\&\quad+\|\delta_t\boldsymbol{e}_0\|_{0,\epsilon}\left(\tau\left\|\partial_t^2\boldsymbol{A}\right\|_{\boldsymbol{L}^\infty(t_0,t_1;\boldsymbol{L}^2(\Omega))}+h^2\left\|\partial_t\boldsymbol{A}_1\right\|_{\boldsymbol{H}^2(\Omega)}\right)\\&\quad+\tau\left(\tau\left\|\partial_t^3\boldsymbol{A}\right\|_{\boldsymbol{L}^\infty(0,T;\boldsymbol{L}^2(\Omega))}+h^2\left\|\partial_{tt}\boldsymbol{A}\right\|_{\boldsymbol{L}^\infty(0,T;\boldsymbol{H}^2(\Omega))}\right)\sum_{k=1}^{n-1}\|\delta_t\boldsymbol{e}_k\|_{0,\epsilon}\\&\lesssim\left(\tau+h^2\right)\left(\|\delta_t\boldsymbol{e}_n\|_{0,\epsilon}^2+\|\delta_t\boldsymbol{e}_0\|_{0,\epsilon}^2\right)+\left(\tau+h^2\right)\left(\sum_{k=1}^n\tau\|\delta_t\boldsymbol{e}_k\|_{0,\epsilon}^2\right)^{1/2}.\end{aligned}\tag{40}$$

Moreover, an application of the Cauchy–Schwarz inequality and (34) leads to

$$\begin{aligned}\sum_{k=1}^n\tau R_k^{(3)}&\lesssim\sum_{k=1}^n\tau\left\|\mathbf{curl}\,\boldsymbol{e}_k\right\|_{0,1/\mu}\left(\tau\left\|\partial_{tt}\boldsymbol{A}\right\|_{\boldsymbol{L}^\infty(t_{k-1},t_k;\boldsymbol{H}(\mathbf{curl},\Omega))}+h\left\|\partial_t\boldsymbol{A}_k\right\|_{\boldsymbol{H}^1(\mathbf{curl},\Omega)}\right)\\&\lesssim\left[\tau\left\|\partial_{tt}\boldsymbol{A}\right\|_{\boldsymbol{L}^\infty(0,T;\boldsymbol{H}(\mathbf{curl},\Omega))}+h\left\|\partial_t\boldsymbol{A}\right\|_{\boldsymbol{L}^\infty(0,T;\boldsymbol{H}^1(\mathbf{curl},\Omega))}\right]\left(\sum_{k=1}^n\tau\left\|\mathbf{curl}\,\boldsymbol{e}_k\right\|_{0,1/\mu}^2\right)^{1/2}.\end{aligned}\tag{41}$$

The estimate of $R_k^{(4)}$ is easy and given by

$$\sum_{k=1}^n\tau R_k^{(4)}\le\sum_{k=1}^n\tau\int_\Omega j_c\left(\boldsymbol{x},t_k\right)\left|\mathcal{I}_h\left(\partial_t\boldsymbol{A}_k\right)-\partial_t\boldsymbol{A}_k\right|\,\mathrm{d}\boldsymbol{x}\lesssim\tau h^2\sum_{k=1}^n\left\|\partial_t\boldsymbol{A}_k\right\|_{\boldsymbol{H}^2(\Omega)}\lesssim h^2.\tag{42}$$

Now it is left to estimate $R_k^{(5)}$. Using (6), (37) and the Cauchy–Schwarz inequality, we obtain

$$\begin{aligned}\sum_{k=1}^{n} \tau R_k^{(5)} &\leq \sum_{k=1}^{n} \tau \left\| \epsilon\, \partial_{tt} \boldsymbol{A}_k + \mathbf{curl}\, \left(\mu^{-1} \mathbf{curl}\, \boldsymbol{A}_k\right) - \boldsymbol{\ell}_k \right\|_0 \|\boldsymbol{\eta}_k\|_0 = \sum_{k=1}^{n} \tau \, \|\boldsymbol{J}_k\|_0 \, \|\boldsymbol{\eta}_k\|_0 \\ &\lesssim h^2 \sum_{k=1}^{n} \tau \|\boldsymbol{J}\|_{L^\infty(0,T;\boldsymbol{L}^2(\Omega))} \, \|\partial_t \boldsymbol{A}_k\|_{\boldsymbol{H}^2(\Omega)} \lesssim h^2, \end{aligned} \tag{43}$$

where we have used the regularity of $\boldsymbol{J}$, c.f. Theorem 1 of [22], Lemma 4.3 of [23] and Lemma 2.1 of [45] for more details.

Finally, inserting (39)–(43) into (33) and assuming $\tau + h \ll 1$, we obtain

$$\|\delta_t \boldsymbol{e}_n\|_{0,\epsilon}^2 + \|\mathbf{curl}\, \boldsymbol{e}_n\|_{0,1/\mu}^2 \lesssim h^2 + (\tau + h) \left(\sum_{k=1}^{n} \tau \left(\|\delta_t \boldsymbol{e}_k\|_{0,\epsilon}^2 + \|\mathbf{curl}\, \boldsymbol{e}_k\|_{0,1/\mu}^2 \right) \right) + \|\delta_t \boldsymbol{e}_0\|_{0,\epsilon}^2 + \|\mathbf{curl}\, \boldsymbol{e}_0\|_{0,1/\mu}^2 .$$

The proof is finished by using (16) and Gronwall's inequality. □

Remark 4.5. We discuss the convergence behaviors from the temporal and spatial aspect, separately. Since we are using the first-order backward time-difference for $\partial_t \boldsymbol{A}$, the first-order convergence rate in time is expected to be optimal for $\|\delta_t(\boldsymbol{A}_k - \boldsymbol{A}_k^h)\|_{0,\epsilon}$, not for $\|\mathbf{curl}\,(\boldsymbol{A}_k - \boldsymbol{A}_k^h)\|_{0,1/\mu}$. However, Theorems 3.3 and 4.4 reveal an optimal spatial error estimate for $\|\mathbf{curl}\,(\boldsymbol{A}_k - \boldsymbol{A}_k^h)\|_{0,1/\mu}$, rather than $\|\delta_t(\boldsymbol{A}_k - \boldsymbol{A}_k^h)\|_{0,\epsilon}$, by using the first-order Nédélec edge elements.

5. Numerical experiments

In this section, we first propose two methods for solving the discrete variational inequality Problem 4.1, then verify the convergence orders and performances of our finite element method with two numerical examples, one has an analytical solution and the other is from the type-II superconductivity. The implementations of our algorithms are based on the finite element software Parallel Hierarchical Grid (PHG) [31, 50]. All computations are carried out on the LSSC-IV Cluster of the State Key Laboratory of Scientific and Engineering Computing, Chinese Academy of Sciences.

5.1. The projection method

The first method is based on the classical projection method, or the Uzawa-type method (cf. [14, 24, 29]). Introduce a Lagrange multiplier $\boldsymbol{\lambda} = -\boldsymbol{J}/j_c$ and define the inner product $(\cdot,\cdot)_{j_c} := (j_c(\boldsymbol{x},t)\,\cdot,\cdot)$. The variational inequality can be reformulated into a variational equation with constraints (cf. [11, 12, 14, 25]).

Problem 5.1. Find $\boldsymbol{A} \in W^{2,\infty}(0,T;\boldsymbol{L}^2(\Omega)) \cap W^{1,\infty}(0,T;\boldsymbol{H}_0(\mathbf{curl}\,,\Omega))$ and $\boldsymbol{\lambda} \in L^\infty(0,T;\boldsymbol{L}^2(\Omega))$ such that

$$\begin{cases} (\epsilon\, \partial_{tt} \boldsymbol{A}, \boldsymbol{v}) + a(\boldsymbol{A}, \boldsymbol{v}) + (\boldsymbol{\lambda}, \boldsymbol{v})_{j_c} = (\boldsymbol{\ell}, \boldsymbol{v}) \quad \forall\, \boldsymbol{v} \in \boldsymbol{H}_0(\mathbf{curl}\,,\Omega), \\ \qquad |\boldsymbol{\lambda}| \leq 1, \quad \boldsymbol{\lambda} \cdot \partial_t \boldsymbol{A} = |\partial_t \boldsymbol{A}| \quad \text{in } \Omega \times (0,T), \end{cases} \tag{44}$$

The finite element space for discretizing $\boldsymbol{\lambda}$ is chosen as the space of piecewise linear and discontinuous polynomials

$$\boldsymbol{\Lambda}_h = \left\{ \boldsymbol{v}_h \in \boldsymbol{L}^2(\Omega) : \boldsymbol{v}_h|_K \in \mathcal{P}_1(K), \quad \forall K \in \mathcal{T}_h \right\}.$$

Similarly, we introduce a discrete Lagrange multiplier and propose the discrete problem.

Problem 5.2. Find $\boldsymbol{A}_k^h \in \boldsymbol{V}_h$ and $\boldsymbol{\lambda}_k^h \in \boldsymbol{\Lambda}_h$ such that

$$\begin{cases} \left(\epsilon\, \delta_{tt} \boldsymbol{A}_k^h, \boldsymbol{v}^h\right) + a\left(\boldsymbol{A}_k^h, \boldsymbol{v}^h\right) + \left(\boldsymbol{\lambda}_k^h, \boldsymbol{v}^h\right)_{j_c} = \left(\boldsymbol{\ell}_k, \boldsymbol{v}^h\right) \quad \forall\, \boldsymbol{v}^h \in \boldsymbol{V}_h, \\ \left|\boldsymbol{\lambda}_k^h\right| \le 1, \quad \boldsymbol{\lambda}_k^h \cdot \delta_t \boldsymbol{A}_k^h = \left|\delta_t \boldsymbol{A}_k^h\right|. \end{cases} \tag{45}$$

The discrete form of $(\cdot,\cdot)_{j_c}$ in (45) contains the value of j_c at t_k.

Algorithm 1. The discrete projection algorithm for solving Problem 5.2.

Step 1. Set the initial guesses $\boldsymbol{\lambda}_{k,0}^h := \boldsymbol{\lambda}_{k-1}^h$, $\boldsymbol{A}_{k,0}^h := \boldsymbol{A}_{k-1}^h$, a parameter $\alpha > 0$, and a tolerance $\varepsilon_{\mathrm{tol}} > 0$.
Step 2. Given $\boldsymbol{\lambda}_{k,n}^h$ with $n \ge 0$, find $\boldsymbol{A}_{k,n+1}^h \in \boldsymbol{V}_h$ which satisfies

$$\left(\epsilon\, \delta_{tt} \boldsymbol{A}_{k,n+1}^h, \boldsymbol{v}^h\right) + a\left(\boldsymbol{A}_{k,n+1}^h, \boldsymbol{v}^h\right) = \left(\boldsymbol{\ell}_k, \boldsymbol{v}^h\right) - \left(\boldsymbol{\lambda}_{k,n}^h, \boldsymbol{v}^h\right)_{j_c}. \tag{46}$$

Step 3. Set $\boldsymbol{\lambda}_{k,n+1}^h = P(\boldsymbol{\lambda}_{k,n}^h + \alpha \delta_t \boldsymbol{A}_{k,n+1}^h)$, where $P(\boldsymbol{\mu}) := \max\left\{-\mathbf{1}, \min\{\mathbf{1}, \boldsymbol{\mu}\}\right\}$.
Step 4. If $\left\|\boldsymbol{A}_{k,n+1}^h - \boldsymbol{A}_{k,n}^h\right\|_0 / \left\|\boldsymbol{A}_{k,n+1}^h\right\|_0 < \varepsilon_{\mathrm{tol}}$, set $\boldsymbol{A}_k^h \leftarrow \boldsymbol{A}_{k,n+1}^h$ and $k \leftarrow k+1$. Otherwise, go to Step 2.

In Algorithm 1, the first-order and second-order time differences are, respectively, defined as follows

$$\delta_t \boldsymbol{A}_{k,n+1}^h = \frac{\boldsymbol{A}_{k,n+1}^h - \boldsymbol{A}_{k-1}^h}{\tau}, \qquad \delta_{tt} \boldsymbol{A}_{k,n+1}^h = \frac{\boldsymbol{A}_{k,n+1}^h - 2\boldsymbol{A}_{k-1}^h + \boldsymbol{A}_{k-2}^h}{\tau^2},$$

which will also be used in the forthcoming regularization method.

5.2. The regularization method

The idea of the regularization method is to polish the nonsmooth functional φ with a small parameter $\varepsilon > 0$ such that the new functional φ_ε is Fréchet-differentiable and transform the variational inequality into a nonlinear variational equation. In our case, the regularized functional is defined by

$$\varphi_\varepsilon(t, w) = \int_\Omega j_c(\boldsymbol{x}, t) \cdot \rho_\varepsilon(w)\, \mathrm{d}\boldsymbol{x}, \qquad \rho_\varepsilon(s) := \sqrt{s^2 + \varepsilon^2} - \varepsilon,$$

then

$$\lim_{h \to 0} \frac{\varphi_\varepsilon(t, w + hv) - \varphi_\varepsilon(t, w)}{h} = (\rho'_\varepsilon(w), \boldsymbol{v})_{j_c}.$$

Following ([11], Chapt. I, 7.1), the finite element approximation to the regularized problem is proposed as follows.

Problem 5.3. Find an element $\boldsymbol{A}_{\varepsilon,k}^h \in \boldsymbol{V}_h$ such that

$$\left(\epsilon\, \delta_{tt} \boldsymbol{A}_{\varepsilon,k}^h, \boldsymbol{v}^h\right) + a\left(\boldsymbol{A}_{\varepsilon,k}^h, \boldsymbol{v}^h\right) + \left(\rho'_\varepsilon\left(\delta_t \boldsymbol{A}_{\varepsilon,k}^h\right), \boldsymbol{v}^h\right)_{j_c} = \left(\boldsymbol{\ell}_k, \boldsymbol{v}^h\right) \quad \forall\, \boldsymbol{v}^h \in \boldsymbol{V}_h. \tag{47}$$

In both algorithms, we need to solve a linearized $\boldsymbol{H}(\mathbf{curl})$-elliptic problem in $\boldsymbol{V}_h$ at each time step and each iteration. For both (46) and (48), the stiff matrices are symmetric and positive definite. We use the preconditioned conjugate gradient (PCG) method to solve the algebraic systems with the Hiptmair-Xu (HX) preconditioner [19, 27].

Remark 5.4. In [16, 17], Yousept *et al.* proposed a leap-frog scheme for the original formulation of Maxwell variational inequalities (1). Compared to the implicit Euler scheme, it turns out to be much more suitable and efficient since an efficiently computable explicit formula is available for the discretized variational inequality. Thus, it is interesting to extend the ideas therein and design appropriate explicit methods. We will envision this in the future work.

Algorithm 2. The Picard iteration for solving Problem 5.3.

Step 1. Set $\boldsymbol{A}_{\epsilon,0}^h = \boldsymbol{A}_0^h$ and $\delta_t \boldsymbol{A}_{\epsilon,0}^h = \tilde{\boldsymbol{E}}_0^h$.

Step 2. Given $\delta_t \boldsymbol{A}_{\varepsilon,k,0}^h := \delta_t \boldsymbol{A}_{\varepsilon,k-1}^h$, find $\boldsymbol{A}_{\varepsilon,k,n+1}^h \in \boldsymbol{V}_h$ $(n \geq 1)$ such that

$$\left(\epsilon\, \delta_{tt} \boldsymbol{A}_{\varepsilon,k,n+1}^h, \boldsymbol{v}^h\right) + a\left(\boldsymbol{A}_{\varepsilon,k,n+1}^h, \boldsymbol{v}^h\right) + \int_\Omega j_c \frac{\delta_t \boldsymbol{A}_{\varepsilon,k,n+1}^h \cdot \boldsymbol{v}^h}{\sqrt{\left|\delta_t \boldsymbol{A}_{\varepsilon,k,n}^h\right|^2 + \varepsilon^2}} \,\mathrm{d}\boldsymbol{x} = \left(\boldsymbol{\ell}_k, \boldsymbol{v}^h\right) \quad \forall \boldsymbol{v}^h \in \boldsymbol{V}_h. \tag{48}$$

Step 3. If $\left\|\boldsymbol{A}_{\varepsilon,k,n+1}^h - \boldsymbol{A}_{\varepsilon,k,n}^h\right\|_0 / \left\|\boldsymbol{A}_{\varepsilon,k,n+1}^h\right\|_0 < \varepsilon_{\mathrm{tol}}$, set $\boldsymbol{A}_{\varepsilon,k}^h := \boldsymbol{A}_{\varepsilon,k,n+1}^h$ and $k \leftarrow k+1$. Otherwise, go to Step 2.

TABLE 1. Convergence orders by Algorithm 1.

(τ, h)	$\left\|\boldsymbol{A}_N - \boldsymbol{A}_N^h\right\|_0$	Order	$\left\|\boldsymbol{A}_N - \boldsymbol{A}_N^h\right\|_{\mathbf{curl},\Omega}$	Order
(τ_0, h_0)	4.84e−03	–	3.57e−02	–
$(\tau_0, h_0)/2$	2.35e−03	1.04	1.82e−02	0.98
$(\tau_0, h_0)/4$	1.25e−03	0.91	9.23e−03	0.98
$(\tau_0, h_0)/8$	6.57e−04	0.93	4.66e−03	0.98
$(\tau_0, h_0)/16$	3.37e−04	0.96	2.35e−03	0.99

5.3. Numerical examples

Without specifications, we set the relative tolerance and the maximal number of iterations for the PCG method by $\varepsilon_{\mathrm{pcg}} = 10^{-9}$ and $N_{\mathrm{pcg}}^{\max} = 100$, and set the relative tolerance and maximal number of iterations for solving the nonlinear problems by $\varepsilon_{\mathrm{tol}} = 10^{-6}$ and $N_{\mathrm{nl}}^{\max} = 100$. The relaxation parameter is set by $\alpha = 1$ for the projection method. The regularization parameter is set by $\varepsilon = 10^{-6}$ for the regularization method.

Example 5.1 (Convergence orders)**.** This example is to verify the convergence orders of the finite element method and investigate the performances for the two solution algorithms. The computational domain is set by $\Omega = (0,1)^3$ and the physical parameters are set by $\epsilon = 1$ and $\mu = 1$. The exact solution is taken as

$$\boldsymbol{A}(\boldsymbol{x}, t) = \mathrm{e}^{-t}(\sin x \cos(yz), \cos x, \sin(yz)\sin x)^\top.$$

The current density is taken as $\boldsymbol{J} = -\partial_t \boldsymbol{A}/|\partial_t \boldsymbol{A}|$ and the critical current is $j_c(\boldsymbol{x}, t) = 1$. The right-hand side $\boldsymbol{\ell}$ and the initial conditions are computed with the explicit expression of $\boldsymbol{A}$. The final time is taken as $T = 1$.

In this example, we employ a sequence of uniform tetrahedral meshes of Ω with the initial mesh size $h_0 = \sqrt{3}/4$ and a sequence of uniform subdivisions of $[0, T]$ with the initial time-step length $\tau_0 = 0.05$. The mesh size and the time-step length satisfy $\tau = O(h)$ at each level. Table 1 shows the convergence orders of the numerical solution $\boldsymbol{A}_N^h$ which is computed with the projection algorithm at the final time. The first-order convergence is obtained for the numerical solution in both $\boldsymbol{L}^2(\Omega)$- and $\boldsymbol{H}(\mathbf{curl}, \Omega)$-norms.

Table 2 shows the convergence orders of $\boldsymbol{A}_N^h$ which are computed with the regularization algorithm at the final time. Again we observe the first-order convergence of the numerical solution in both $\boldsymbol{L}^2(\Omega)$- and $\boldsymbol{H}(\mathbf{curl}, \Omega)$-norms. The numerical results verify the theoretical analysis in Theorem 4.4.

To compare the performances of the two algorithms, we further present the number of nonlinear iterations N_{nl} and average number of iterations of the PCG method, N_{pcg}, for solving linear algebraic systems arising from Algorithms 1 and 2. From Table 3, we find that the regularization method needs much less iterations than the projection method. An interesting phenomenon shows that both N_{nl} and N_{pcg} decrease with respect to τ and h. This is mainly due to the fact that the discrete problem usually has better condition number for smaller τ than a larger one. Moreover, on each mesh level, the average number of PCG iterations for Algorithm 1 is

TABLE 2. Convergence orders by Algorithm 2.

(τ, h)	$\left\Vert \boldsymbol{A}_N - \boldsymbol{A}_N^h \right\Vert_0$	order	$\left\Vert \boldsymbol{A}_N - \boldsymbol{A}_N^h \right\Vert_{\mathbf{curl}}$	order
(τ_0, h_0)	4.49e−03	–	3.59e−02	–
$(\tau_0, h_0)/2$	2.32e−03	0.95	1.82e−02	0.98
$(\tau_0, h_0)/4$	1.25e−03	0.90	9.24e−03	0.98
$(\tau_0, h_0)/8$	6.56e−04	0.93	4.66e−03	0.99
$(\tau_0, h_0)/16$	3.37e−04	0.96	2.35e−03	0.99

TABLE 3. Numbers of nonlinear iterations and PCG iterations for both the projection method and regularization method at $t = T$.

(τ, h)	Projection method $N_{\rm nl}$ ($N_{\rm pcg}$)	Regularization method $N_{\rm nl}$ ($N_{\rm pcg}$)
(τ_0, h_0)	13 (14)	5 (14)
$(\tau_0, h_0)/2$	7 (14)	4 (12)
$(\tau_0, h_0)/4$	5 (11)	3 (11)
$(\tau_0, h_0)/8$	5 (11)	2 (12)
$(\tau_0, h_0)/16$	5 (9)	2 (10)

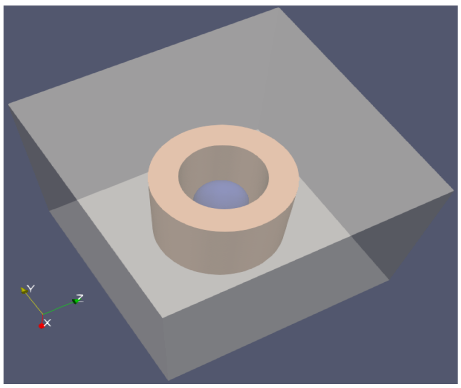

FIGURE 1. An illustration of the coil and superconductor.

very close to that for Algorithm 2. This indicates that the extra term in the regularization method does not affect the efficiency of algebraic solvers remarkably.

Example 5.2 (Type-II superconductivity)**.** In this example, we simulate the physical phenomena of type-II superconductivity. The computational domain is chosen as $\Omega = (-1,1)^3$. The right-hand side represents a circular current carried in a cylindrical pipe $\Omega_p := \left\{\boldsymbol{x} \in \mathbb{R}^3 : |x_1| \le 0.5,\ 0.09 \le x_2^2 + x_3^2 \le 0.25\right\}$,

$$\boldsymbol{\ell}(\boldsymbol{x}) = \begin{cases} \left(x_2^2 + x_3^2\right)^{-1/2} (0, x_3, -x_2)^\top & \text{if } \boldsymbol{x} \in \Omega_p, \\ 0 & \text{if } \boldsymbol{x} \notin \Omega_p. \end{cases}$$

The superconductor $\Omega_{\rm sc} \subset \Omega$ is a ball centered at the origin with a radius $r_{\rm sc} = 0.2$. Figure 1 displays an illustration of the structure. The material parameters are taken as $\epsilon = 1$ and $\mu = 1$. The tetrahedral mesh

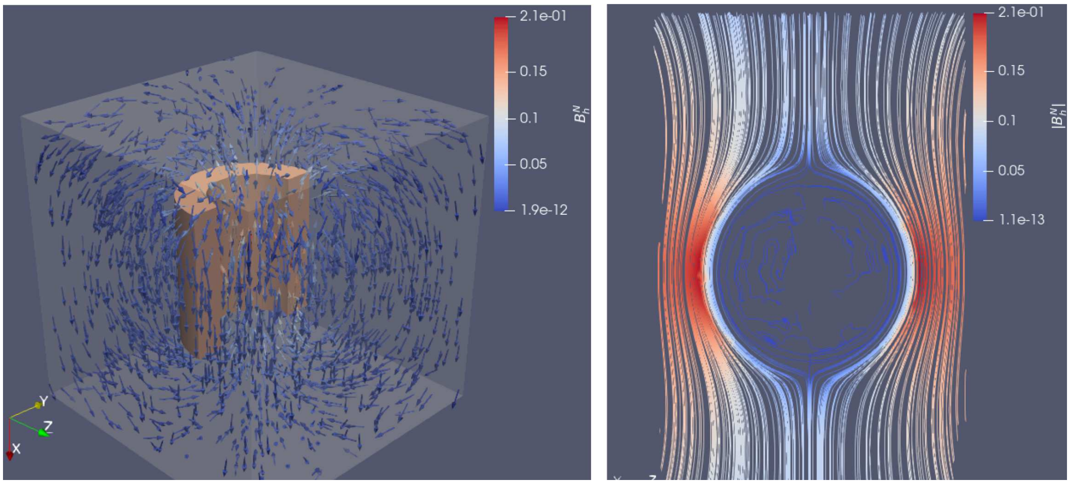

FIGURE 2. *Left*: the distribution of the magnetic field and the clipped pipe coil. *Right*: 2D-slice of the magnetic field lines.

consists of 1 252 352 elements and 2 937 704 degrees of freedom. For the sake of simplicity, we only focus on the regularization method.

The critical current $j_c \equiv 80$ in Ω_{sc} and $j_c \equiv 0$ elsewhere. The final time is set by $T = 1$ and the initial values are set by $\boldsymbol{A}_0 = \mathbf{0}$ and $\boldsymbol{E}_0 = \mathbf{0}$. Figure 2 exhibits magnetic field lines drawn with $\boldsymbol{B}_N^h = \mathbf{curl}\,\boldsymbol{A}_N^h$. The right figure shows clearly that magnetic field lines are repelled by the superconductor. They are squashed between the superconductor and the coil, and the field strength becomes very strong in this area. This physical phenomenon is known as the Meissner–Ochsenfeld effect [41].

Figure 3 shows the effect of the critical current on the magnetic field. As the value of critical current decreases, the magnetic field lines in the squashed area begin to penetrate the superconductor. When the critical current reaches the threshold value 0.1, the magnetic field completely penetrates the superconductor and the Meissner–Ochsenfeld effect disappears. These numerical results are similar to the results presented in [41–43], qualitatively.

6. Conclusion and future work

This work is devoted to the numerical analysis of a hyperbolic Maxwell variational inequality (VI) based on the variable of magnetic vector potential $\boldsymbol{A}$. We study the well-posedness, establish error estimates, propose the classical projection method and the regularization method for solving the $\boldsymbol{A}$-formation of Maxwell VI. We also carry out some numerical tests to confirm the theoretical convergence and the physical phenomena of type-II superconductivity. In [16, 17], the authors propose the mixed finite element methods based on leapfrog time-stepping, which turns out to be much more efficient without additional nonlinear or projection terms in the numerical realization. This will inspire us to investigate appropriate explicit methods for the $\boldsymbol{A}$-formation of Maxwell VI and hemi-VI problems in the future work.

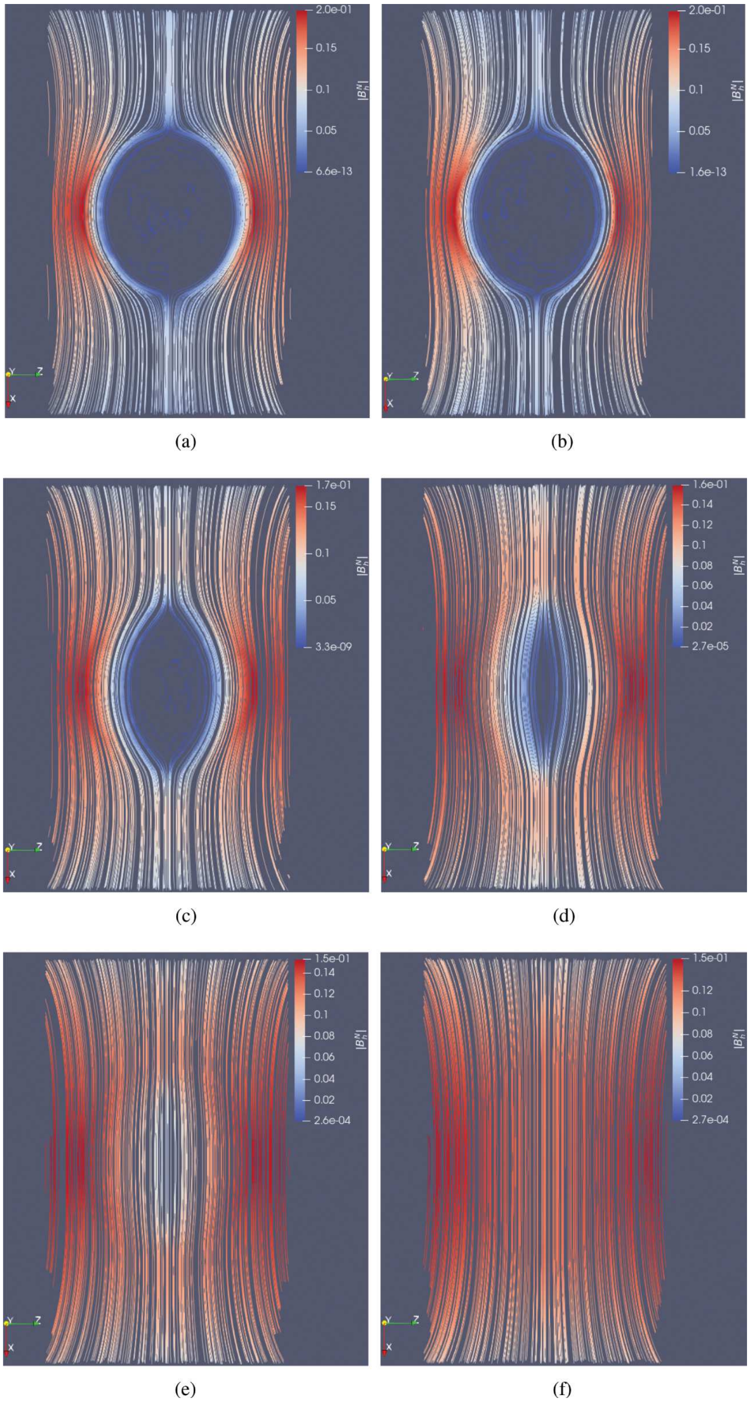

FIGURE 3. Magnetic field lines on a 2D slice obtained with different critical currents. (a) $j_c = 10$. (b) $j_c = 5$. (c) $j_c = 2$. (d) $j_c = 1$. (e) $j_c = 0.5$. (f) $j_c = 0.1$.

Acknowledgments

The authors would like to acknowledge the anonymous reviewers for their constructive and valuable suggestions to improve the quality of this work. This work was partially supported by the Strategic Priority Research Program of the Chinese Academy of Sciences (Nos. XDB0640000, XDB0640100), National Natural Science Foundation of China (Nos. 12371407, 12201575) and Key Scientific Research Project of Colleges and Universities of Henan Province of China (No. 24A110011).

Data availability statement

The research data associated with this article are included in the article.

References

[1] V. Barbu, Optimal Control of Variational Inequalities. Pitman (Advanced Publishing Program), Boston, MA (1984).

[2] J.W. Barrett and L. Prigozhin, Bean's critical-state model as the $p \to \infty$ limit of an evolutionary p-Laplacian equation. *Nonlinear Anal.* **42** (2000) 977–993.

[3] J.W. Barrett and L. Prigozhin, Dual formulations in critical state problems. *Interf. Free Bound.* **8** (2006) 349–370.

[4] J.W. Barrett and L. Prigozhin, A quasi-variational inequality problem in superconductivity. *Math. Models Methods Appl. Sci.* **20** (2010) 679–706.

[5] J.W. Barrett and L. Prigozhin, Existence and approximation of a mixed formulation for thin film magnetization problems in superconductivity. *Math. Models Methods Appl. Sci.* **24** (2014) 991–1015.

[6] J.W. Barrett and L. Prigozhin, Sandpiles and superconductors: nonconforming linear finite element approximations for mixed formulations of quasi-variational inequalities. *IMA J. Numer. Anal.* **35** (2015) 1–38.

[7] C.P. Bean, Magnetization of hard superconductors. *Phys. Rev. Lett.* **8** (1962) 250–253.

[8] C.P. Bean, Magnetization of high-field superconductors. *Rev. Mod. Phys.* **36** (1964) 31–39.

[9] G. Caselli, M. Hensel and I. Yousept, Quasilinear variational inequalities in ferromagnetic shielding: well-posedness, regularity, and optimal control. *SIAM J. Control Optim.* **61** (2023) 2043–2068.

[10] S.S. Dragomir, Some Gronwall Type Inequalities and Applications. Nova Science Publishers, Inc., Hauppauge, NY, 2003.

[11] G. Duvaut and J.L. Lions, Inequalities in Mechanics and Physics. Springer-Verlag, Berlin (1976).

[12] H. Fujita, A coherent analysis of Stokes flows under boundary conditions of friction type. *J. Comput. Appl. Math.* **149** (2002) 57–69.

[13] V. Girault and P.A. Raviart, Finite Element Methods for Navier–Stokes Equations. Theory and Algorithms. Vol. 5 of *Springer Series in Computational Mathematics*. Springer-Verlag, Berlin (1986).

[14] R. Glowinski, J. Lions and R. Tremolieres, Numerical Analysis of Variational Inequalities. Elsevier Science Ltd, North-Holland (1981).

[15] W. Han, M. Ling and F. Wang, Numerical solution of an H(curl)-elliptic hemivariational inequality. *IMA J. Numer. Anal.* **43** (2023) 976–1000.

[16] M. Hensel and I. Yousept, Numerical analysis for Maxwell obstacle problems in electric shielding. *SIAM J. Numer. Anal.* **60** (2022) 1083–1110.

[17] M. Hensel, M. Winckler and I. Yousept, Numerical solutions to hyperbolic Maxwell quasi-variational inequalities in Bean–Kim model for type-II superconductivity. *ESAIM Math. Model. Numer. Anal.* **58** (2024) 1385–1411.

[18] R. Hiptmair, Finite elements in computational electromagnetism. *Acta Numer.* **11** (2002) 237–339.

[19] R. Hiptmair and J. Xu, Nodal auxiliary space preconditioning in $\mathbf{H}(\mathbf{curl})$ and $\mathbf{H}(\mathrm{div})$ spaces. *SIAM J. Numer. Anal.* **45** (2007) 2483–2509.

[20] R. Hiptmair, L.X. Li, S.P. Mao and W.Y. Zheng, A fully divergence-free finite element method for magnetohydrodynamic equations. *Math. Models Methods Appl. Sci.* **28** (2018) 659–695.

[21] K.B. Hu, Y.C. Ma and J. Xu, Stable finite element methods preserving $\nabla \cdot \boldsymbol{B} = 0$ exactly for MHD models. *Numer. Math.* **135** (2017) 371–396.

[22] F. Jochmann, On a first-order hyperbolic system including Bean's model for superconductors with displacement current. *J. Differ. Equ.* **246** (2009) 2151–2191.

[23] F. Jochmann, Well-posedness for Bean's critical state model with displacement current. *J. Math. Anal. Appl.* **362** (2010) 505–513.

[24] T. Kashiwabara, On a finite element approximation of the Stokes equations under a slip boundary condition of the friction type. *Jpn. J. Ind. Appl. Math.* **30** (2013) 227–261.

[25] N. Kikuchi and J.T. Oden, Contact Problems in Elasticity: A Study of Variational Inequalities and Finite Element Methods. SIAM, Philadelphia (1988).
[26] Y.B. Kim, C.F. Hempstead and A.R. Strnad, Magnetization and critical supercurrents. *Phys. Rev.* **129** (1963) 528–535.
[27] T.V. Kolev and P.S. Vassilevski, Parallel auxiliary space AMG for H(curl) problems. *J. Comput. Math.* **27** (2009) 604–623.
[28] A. Laurain, M. Winckler and I. Yousept, Shape optimization for superconductors governed by H(curl)-elliptic variational inequalities. *SIAM J. Control Optim.* **59** (2021) 2247–2272.
[29] Y. Li and K.T. Li, Uzawa iteration method for Stokes type variational inequality of the second kind. *Acta. Math. Appl. Sin.* **17** (2011) 303–316.
[30] J.L. Lions and G. Stampacchia, Variational inequalities. *Commun. Pure Appl. Math.* **20** (1967) 493–519.
[31] H. Liu and L.B. Zhang, Parallel implementation of commonly used marking strategies in the adaptive finite element toolbox PHG. *J. Numer. Methods Comput. Appl.* **30** (2009) 315–320.
[32] A. Milani, On a variational inequality with time dependent convex constraints for the Maxwell equations. *Rend. Sem. Mat. Univ. Politec. Torino* **36** (1979) 389–401.
[33] A. Milani, On a variational inequality with time dependent convex constraint for the Maxwell equations. *Rend. Sem. Mat. Univ. Politec. Torino* **43** (1985) 171–183.
[34] F. Miranda, J.-F. Rodrigues and L. Santos, A class of stationary nonlinear Maxwell systems. *Math. Models Methods Appl. Sci.* **19** (2009) 1883–1905.
[35] F. Miranda, J.-F. Rodrigues and L. Santos, On a p-curl system arising in electromagnetism. *Discrete Contin. Dyn. Syst. Ser. S* **5** (2012) 605–629.
[36] F. Miranda, J.-F. Rodrigues and L. Santos, Evolutionary quasi-variational and variational inequalities with constraints on the derivatives. *Adv. Nonlinear Anal.* **9** (2020) 250–277.
[37] P. Monk, Finite Element Methods for Maxwell's Equations. *Numerical Analysis and Scientic Computation.* Clarendon Press (2003).
[38] L. Prigozhin, On the Bean critical-state model in superconductivity. *Eur. J. Appl. Math.* **7** (1996) 237–247.
[39] L. Prigozhin, The Bean model in superconductivity: variational formulation and numerical solution. *J. Comput. Phys.* **129** (1996) 190–200.
[40] L. Prigozhin, Variational inequalities in critical-state problems. *Phys. D: Nonlinear Phenom.* **197** (2004) 197–210.
[41] M. Winckler and I. Yousept, Fully discrete scheme for Bean's critical-state model with temperature effects in superconductivity. *SIAM J. Numer. Anal.* **57** (2019) 2685–2706.
[42] M. Winckler and I. Yousept, Maxwell variational inequalities in type-II superconductivity. *Int. Ser. Numer. Math.* **172** (2022) 499–519.
[43] M. Winckler, I. Yousept and J. Zou, Adaptive edge element approximation for H(curl) elliptic variational inequalities of second kind. *SIAM J. Numer. Anal.* **58** (2020) 1941–1964.
[44] I. Yousept, Optimal control of quasilinear H(curl)-elliptic partial differential equations in magnetostatic field problems. *SIAM J. Control Optim.* **5** (2013) 3624–3651.
[45] I. Yousept, Hyperbolic Maxwell variational inequalities for Bean's critical-state model in type-II superconductivity. *SIAM J. Numer. Anal.* **55** (2017) 2444–2464.
[46] I. Yousept, Optimal control of non-smooth hyperbolic evolution maxwell equations in type-II superconductivity. *SIAM J. Control Optim.* **55** (2017) 2305–2332.
[47] I. Yousept, Hyperbolic Maxwell variational inequalities of the second kind. *ESAIM Control Optim. Calc. Var.* **26** (2020) 34.
[48] I. Yousept, Well-posedness theory for electromagnetic obstacle problems. *J. Differ. Equ.* **269** (2020) 8855–8881.
[49] I. Yousept, Maxwell quasi-variational inequalities in superconductivity. *ESAIM Math. Model. Numer. Anal.* **55** (2021) 1545–1568.
[50] L.B. Zhang, T. Cui and H. Liu, A set of symmetric quadrature rules on triangles and tetrahedra. *J. Comput. Math.* **27** (2009) 89–96.